frontiers | Frontiers in Marine Science

TYPE Original Research
PUBLISHED 02 November 2022
DOI 10.3389/fmars.2022.911522

OPEN ACCESS

EDITED BY
Linda Wegley Kelly,
Scripps Institution of Oceanography, University of California, United States

REVIEWED BY
Wee Cheah,
University of Malaya, Malaysia
Ana Paula B. Moreira,
Federal University of Rio de Janeiro, Brazil

*CORRESPONDENCE
David J. Kieber
djkieber@esf.edu

†PRESENT ADDRESS
Stephanie G. Gardner,
Centre for Marine Science and Innovation, University of New South Wales Sydney, NSW, Australia

SPECIALTY SECTION
This article was submitted to Coral Reef Research, a section of the journal Frontiers in Marine Science

RECEIVED 02 April 2022
ACCEPTED 27 September 2022
PUBLISHED 02 November 2022

CITATION
Xue L, Kieber DJ, Masdeu-Navarro M, Cabrera-Brufau M, Rodríguez-Ros P, Gardner SG, Marrasé C and Simó R (2022) Concentrations, sources, and biological consumption of acrylate and DMSP in the tropical Pacific and coral reef ecosystem in Mo'orea, French Polynesia. *Front. Mar. Sci.* 9:911522. doi: 10.3389/fmars.2022.911522

Concentrations, sources, and biological consumption of acrylate and DMSP in the tropical Pacific and coral reef ecosystem in Mo'orea, French Polynesia

Lei Xue[1], David J. Kieber[1]*, Marta Masdeu-Navarro[2], Miguel Cabrera-Brufau[2], Pablo Rodríguez-Ros[2], Stephanie G. Gardner[2†], Cèlia Marrasé[2] and Rafel Simó[2]

[1]Department of Chemistry, State University of New York, College of Environmental Science and Forestry, Syracuse, NY, United States, [2]Department of Marine Biology and Oceanography, Institut de Ciències del Mar (ICM-CSIC), Barcelona, Spain

Shallow-water coral reefs hold large quantities of acrylate and its precursor dimethylsulfoniopropionate (DMSP), but production and removal processes for these compounds are poorly characterized. Here we determined the concentrations and cycling of acrylate and DMSP in a transect from a coral reef ecosystem to the open ocean, 2 km beyond the reef in Mo'orea, French Polynesia, during April 2018. Concentrations of dissolved acrylate and DMSP were low throughout the reef-ocean transect, ranging from 0.8–3.9 nM and 0.2–3.0 nM, respectively, with no difference observed between the coral reef and open ocean when comparing mean concentrations (± std dev) of dissolved acrylate (1.7 ± 0.7 vs 2.3 ± 0.8 nM) or DMSP (0.9 ± 0.7 vs 1.3 ± 0.6 nM). In the coral reef, dissolved acrylate was rapidly taken up by the heterotrophic community with a fast turnover time averaging ~ 6 h, six times faster than in the open ocean, and nearly as fast as the average turnover time of dissolved DMSP (~ 3 h). A clear diel trend was observed for the heterotrophic consumption of dissolved acrylate and DMSP in the coral reef, with higher uptake rate constants during daylight hours, synchronized with the larger daytime release of acrylate and DMSP from the coral compared to the nighttime release of these compounds. We also measured photochemical production rates of acrylate in Mo'orean waters, but rates were one to two orders of magnitude slower compared to its rates of biological consumption. Coral and macroalgae were the main sources of dissolved acrylate and DMSP to the reef ecosystem. Our results indicate there is rapid turnover of acrylate and DMSP in the coral reef with a tight coupling between production and removal pathways that maintain dissolved concentrations of these two

compounds at very low levels. These algal and coral-derived substrates serve as important chemical links between the coral and heterotrophic communities, two fundamental components in the ecological network in coral reefs.

KEYWORDS

acrylic acid, photochemistry, acropora, symbiodiniaceae, dimethylsulfoxide, DMSO, pocillopora, turbinaria

Introduction

Acrylate is produced through the enzymatic cleavage of DMSP, an organosulfur metabolite produced by many marine phytoplankton including the endosymbiotic dinoflagellates found in shallow reef-building coral. These dinoflagellates are some of the largest DMSP producers in the world's oceans (Keller, 1989; Caruana and Malin, 2014), with high cell densities in the coral host, rivaling those recorded for planktonic dinoflagellates during an algal bloom (Drew, 1972; Van Alstyne et al., 2006). DMSP is also detected in large quantities in the tissues and mucus of many coral species (Hill et al., 1995; Broadbent et al., 2002; Yost and Mitchelmore, 2010; Swan et al., 2017; Haydon et al., 2018) and giant clams (Hill et al., 2000; Van Alstyne et al., 2006; Guibert et al., 2020). Additionally, both the coral host (Raina et al., 2013) and its associated bacteria (Curson et al., 2017) can produce DMSP. Therefore, coral reef systems are prodigious producers of DMSP, with most of the DMSP production occurring in association with the coral and not in the water column.

DMSP lyases, which catalyze the conversion of DMSP to acrylate and dimethylsulfide (DMS) in equimolar quantities, has been detected in the coral endosymbiotic dinoflagellate Symbiodiniaceae (Yost and Mitchelmore, 2009; Caruana and Malin, 2014), suggesting that high concentrations of acrylate should also be present in the coral holobiont. Indeed, in a prevalent Great Barrier Reef coral, *Acropora millepora*, Tapiolas et al. (2010) determined that acrylate constituted 13–15% of the total carbon in the organic extract of the *A. millepora* holobiont. A subsequent survey observed high concentrations of acrylate in sixteen reef-building coral, with some of them showing acrylate concentrations comparable to or even higher than those of its precursor DMSP (Tapiolas et al., 2013).

Acrylate and DMSP are proposed to serve as antioxidants in coral (Yost et al., 2010; Raina et al., 2013; Deschaseaux et al., 2014; Gardner et al., 2016; Gardner et al., 2017), a function first proposed for these metabolites in microalgae (e.g., Sunda et al., 2002; Kinsey et al., 2016) and benthic macroalgae (Burdett et al., 2012; Kerrison et al., 2012; Rix et al., 2012). This function would not be surprising since corals are exposed to a diverse range of environmental stressors daily (e.g., high light, hypersalinity, air exposure) that can induce high levels of oxidative stress and the production of cell-damaging reactive oxygen species (ROS) including superoxide and hydroxyl radicals (Hoegh-Guldberg, 1999). When juveniles and adult colonies of *A. millepora* and *A. tenuis* were thermally stressed, Raina et al. (2013) observed a significant increase in DMSP and decrease in cellular acrylate concentrations. Gardner et al. (2016) observed a significant decrease in cellular DMSP and corresponding increase in the ratio of dimethylsulfoxide (DMSO) to DMSP in *A. millepora* under hyposaline conditions. While these studies showed different responses, both are consistent with acrylate and DMSP serving as de facto antioxidants in the coral holobiont during periods of low or high oxidative stress. In this capacity, cellular concentrations of acrylate and DMSP do not need to be actively controlled because their concentrations are many orders of magnitude higher than expected ROS levels. Instead, other physiological functions will control cellular concentrations of DMSP and acrylate including osmotic regulation or carbon overflow (Kinsey et al., 2016). In addition to the potential role in removing ROS in coral tissue or the mucus where acrylate concentrations are expected to be substantial (Broadbent and Jones, 2004; Tapiolas et al., 2010; Tapiolas et al., 2013), acrylate may play an antimicrobial role preventing the colonization of pathogenic bacteria (Raina et al., 2010), similar to the antiviral function proposed for acrylic acid in the microalgae *Emiliania huxleyi* (Evans et al., 2006; Evans et al., 2007).

Zooplankton grazing, cell lysis, algal exudation, and viral infection release particulate acrylate ($acrylate_p$) and DMSP ($DMSP_p$) from marine phytoplankton into the dissolved phase, where these compounds are largely consumed by the heterotrophic bacteria. Tyssebotn et al. (2017) determined that acrylate was readily consumed by microbes in the Gulf of Mexico at a rate between 0.07 and 1.8 nM d^{-1}, with a significant fraction of the acrylate assimilated into macromolecules or respired to CO_2. However, the contribution of acrylate to bacterial carbon demand in the Gulf of Mexico was negligible, ranging from 0.013 to 0.13% (Tyssebotn et al., 2017), and the turnover of acrylate was relatively slow (median 4.8 d) compared to the turnover of DMSP (median 3.1 h). In contrast to acrylate, the crucial role of DMSP as a source of reduced sulfur and carbon for marine bacteria is well documented (e.g., Kiene and Linn, 2000a; Simó

et al., 2002; Vila-Costa et al., 2007; Levine et al., 2016; Motard-Côté et al., 2016; Lizotte et al., 2017; Kiene et al., 2019). Corals can expel ~10% of their algal symbionts on a daily basis and even more when they are physically or chemically stressed (Broadbent and Jones, 2006), with the expelled Symbiodiniaceae exposed to stress and mortality similar to planktonic phytoplankton. This may result in releases of large quantities of DMSP and acrylate (Masdeu-Navarro et al., 2022) that will feed the fast microbial cycling of dissolved carbon and sulfur in the coral reef.

Acrylate and DMS are produced in equimolar quantities from the enzymatic lysis of DMSP by lyases. However, while DMS has been studied extensively in the global oceans including in coral reefs (Jones et al., 2018; Jackson et al., 2020) due to its potential role in regulating the Earth's radiation budget and climate (Charlson et al., 1987), only a few studies have examined the cycling and ecological impacts of acrylate in coral reefs beyond the impacts to the coral holobiont. In this study, we demonstrate that (1) both acrylate and DMSP are rapidly consumed by planktonic microbes once released into the dissolved phase, and (2) the consumption of dissolved acrylate and DMSP exhibit diel patterns in phase with their release from the coral holobiont.

Materials and methods

Study area

The main field study was conducted from April 4 to 27, 2018 in a coral reef offshore from the Richard Gump South Pacific Research Station located next to Cook's Bay (also known as Paopao Bay) on the northern shore of Mo'orea, French Polynesia (Figure 1). Mo'orea is a volcanic island surrounded by barrier reefs extending outward from the shoreline, creating an extensive semi-enclosed lagoonal system. The typical reef zonation consists of a shallow lagoon that includes a channel, fringing reef and a shallow back reef platform, and an outer fore reef that separates the lagoon from the open ocean (Leichter et al., 2013). The fore reef drops steeply from the near-sea surface to > 500 m over a distance of ~1 km. The shallow fore reef is nearly continuously covered by branching coral colonies of *Pocillopora* sp. and *Acropora* sp. (Adjeroud, 1997). The benthic community on the shallow back reef is composed of turf and fleshy macroalgae and patches of hermatypic corals surrounded by sandy-bottom open areas (http://mcr.lternet.edu/data), with an increasing proportion of

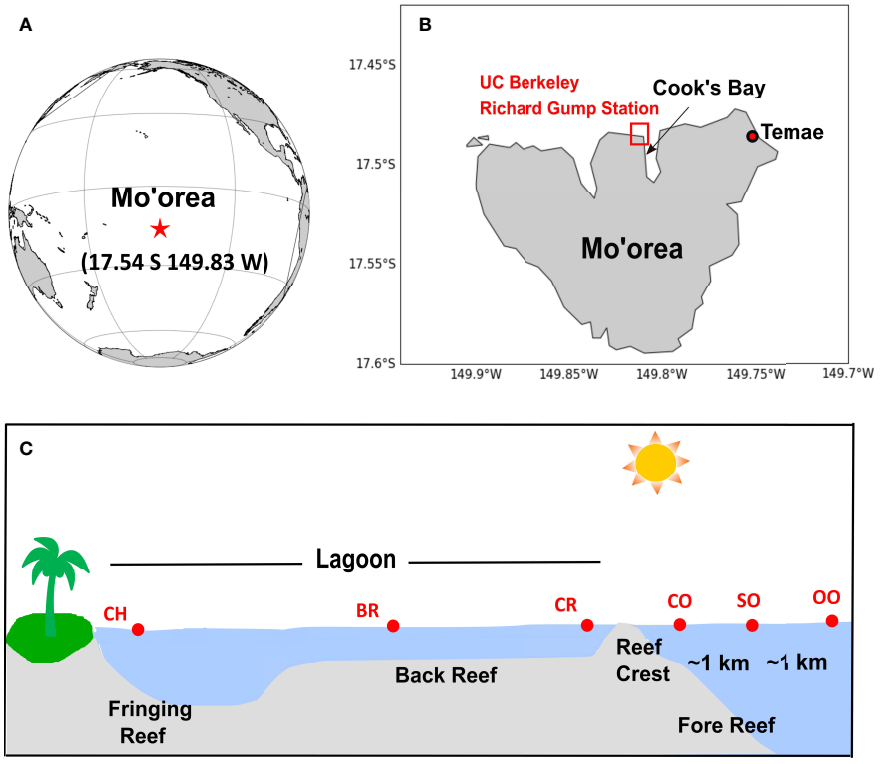

FIGURE 1
Locations of **(A)** the island of Mo'orea, in the South Pacific Ocean, **(B)** the Temae Park coral reef, and the UC Berkeley's Richard Gump Research Station and coral reef where most of the work reported here was conducted, and **(C)** schematic showing the Mo'orea coral reef and reef-ocean transect sampling stations: nearshore outflow channel (CH), back reef (BR), reef crest (reef side of the reef crest, CR), ocean crest (ocean side of the reef crest, CO, ~300 m away from station CR), shelf ocean (SO, ~1 km away from CO), and open ocean (OO, ~2 km away from CO). Note that distances between stations are not drawn to scale. Panel **(C)** was adapted with permission from Leichter et al. (2013).

sandy bottom as one moves shoreward towards the fringe reef and channel. Water movement in the back reef is relatively low from waves, and pass and lagoonal circulation, with flushing times of a few hours to more than day depending on winds and wave energy beyond the reef (Hench et al., 2008; Herdman et al., 2015). Although we did not measure wind speeds or wave heights, qualitatively conditions were calm in the lagoon with no storms or significant wave heights noted during the field study.

Six stations were sampled repeatedly over a three-week period as part of a coral reef-ocean transect study (Figure 1). The six stations included the nearshore outflow channel (CH), the back reef (BR), the reef crest (the reef side of the reef crest, CR), the ocean crest (the ocean side of the reef crest, CO), the shelf ocean (SO, ~1 km from CO), and the open ocean (OO, ~2 km away from CO); these stations correspond to some of the same sampling stations occupied by the Moorea Coral Reef Long Term Ecological Research (MCR LTER) project (Leichter et al., 2013). To assess potential sources of dissolved acrylate and DMSP to the coral reef, an ancillary study was conducted in a coral reef offshore of Temae Beach along the northeastern coast Mo'orea (17.501°S, 149.759°E, Figure 1). The Temae coral reef is a lagoonal system similar to our main study site off Cook's Bay. Two photos depicting typical intermittent reef patches surrounded by sandy bottom present in the Mo'orea coral reef lagoonal system at station BR and the Temae coral reef are shown in Figure S1. A google map showing an aerial overview of the island of Mo'orea and the study area is presented in our companion paper, along with photos showing our protocol used to collect samples close to the coral colonies (Masdeu-Navarro et al., 2022).

Sample collection and storage

Water samples from the near sea surface (~30 cm deep) were collected in precleaned 1, 2, or 8 L opaque (brown) polypropylene bottles from repeated sampling trips to the six stations along a reef-ocean transect (Figure 1). Diel sampling was carried out over a 30-hour period in the back reef (April 12–13) and open ocean stations (April 19–20). A surface microlayer sample was collected in the back reef on April 18 using a glass plate to preliminarily evaluate the potential enrichment and photochemical reactivity of the microlayer sample with respect to acrylate photoproduction compared to the underlying seawater. A bulk seawater sample from ~30 cm below the sea surface was collected in parallel with a precleaned air-tight, all-glass syringe (Hamilton) fitted with 0.32 cm OD Teflon tubing attached to the syringe using a polycarbonate luer-lock, 3-way valve fitting.

To collect samples for dissolved concentrations, each of the aforementioned samples was gravity filtered through a precombusted GF/F filter (25 mm diameter, Whatman) into a precleaned 20 mL scintillation vial following the procedure of small-volume drip filtration (Kiene and Slezak, 2006). Paired with each dissolved sample, another set of samples was collected for the measurement of total concentrations by pipetting 15 mL of unfiltered seawater into a 20 mL scintillation vial. All samples were microwaved to boiling (ca. ~12–15 sec; Kinsey and Kieber, 2016). After samples cooled to room temperature, both dissolved and total samples were bubbled for ~10 min using high-purity nitrogen gas followed by acidification with 150 µL of Ultrex HCl. Each sample was collected in duplicate and was stored at room temperature in the dark until analysis in Syracuse NY. Details regarding chemical sources and purity, and glassware cleaning procedures can be found in the Supplemental Material (SM).

Photochemical experiments

Experiments were performed to determine the photochemical production rate of acrylate in freshly collected 0.2 µm-filtered seawater. Photolysis experiments were conducted with seawater collected from the back reef (station BR), the sea surface microlayer in the back reef, and the open ocean (station OO). After a seawater sample was collected in an 8 L polypropylene bottle, it was gravity filtered through a precleaned 0.2 µm Polycap AS 75 Nylon filter (Whatman) into a precleaned 2.5 L Qorpak glass bottle.

In preparation for a photochemical experiment, the filtered seawater was slowly drawn from the 2.5 L glass bottle into several Teflon-sealed quartz tubes (with no headspace) according to the procedure outlined in Kieber et al. (1997). One set of four quartz tubes was submerged in a 3 cm-deep circulating water bath (28–30 °C) for exposure to sunlight, and a second set of four quartz tubes was wrapped in several layers of aluminum foil and placed in the water bath as dark controls. To obtain sufficient production of acrylate for HPLC analysis, samples from the coral reef and open ocean were exposed to solar radiation for a total of ~15 h and 20 h, respectively, over a two to three-day period. At the end of each experiment, a 10 mL sample was collected in triplicate from each quartz tube, and each 10 mL aliquot was dispensed into a precleaned 20 mL scintillation vial. Samples were subsequently acidified using 100 µL of Ultrex HCl and stored at room temperature in the dark until analysis in Syracuse, NY.

Samples were also collected from the quartz tubes at the beginning and end of each photochemical experiment to determine the absorption spectrum of chromophoric dissolved organic matter (CDOM) in the sunlight-exposed samples and dark controls. Details of the CDOM absorption measurements are given in section CDOM Absorbance.

Triplicate nitrate and nitrite actinometer solutions in 5 mL borosilicate vials were exposed to sunlight along with the quartz tubes to determine the photon exposure between 311 and 333 nm and 330 and 380 nm, respectively, using the methods outlined in

Jankowski et al. (1999) and Kieber et al. (2007). Borosilicate vials for both actinometers were enclosed in neutral-density screening with a percent transmission of 31%. The nitrite actinometer vials were also wrapped with Mylar D film (Jankowski et al., 2000). Dark actinometry controls were wrapped with several layers of aluminum foil, without screening or Mylar D film. Actinometry samples were analyzed at the Gump Research Station by batch fluorescence using a Horiba Aqualog Fluorometer calibrated with salicylic acid standards prepared in a pH 7.2, 2.5 mM sodium bicarbonate solution.

Biological consumption experiments

Time-course incubations were performed to determine biological consumption rates of dissolved acrylate ($acrylate_d$) and DMSP ($DMSP_d$) in unfiltered seawater samples collected from the back reef, station BR, and open ocean, station OO. To perform an incubation for acrylate consumption, 150 µL aliquots of an acrylate standard prepared from DMSP (Xue and Kieber, 2021) were added to unfiltered water samples in triplicate 250 mL polycarbonate (PC) bottles, yielding an initial concentration of ~15 nM for $acrylate_d$ in each bottle. Prior to filling the PC bottles with seawater, they were rinsed several times with Milli-Q water and the unfiltered seawater. The PC bottles were gently inverted several times to mix the added acrylate. Another set of three PC bottles received no added acrylate. Once samples were prepared, they were placed in a large, covered incubator with hosing to continually pump ambient surface seawater through the incubator to maintain the temperature at ~28 °C. All incubations were conducted in the dark. Subsamples were collected from each PC bottle at four separate times during an incubation. The total length of each incubation was 14 h for the coral reef waters and 18 h for the open ocean samples. For each time point, 15 mL subsamples were collected in triplicate from each bottle and processed as discussed below.

The biological consumption of $DMSP_d$ was determined using the glycine betaine (GBT) inhibition method outlined in Kiene and Gerard (1995). Briefly, six precleaned 250 mL PC bottles were filled with freshly collected, unfiltered seawater. Three bottles were treated with 10 µM GBT and three PC bottles were left untreated. All samples were incubated in the dark in the same incubator used for the acrylate incubations. At several time points during an incubation, subsamples from each bottle were collected and processed as outlined below. An additional time-course experiment was performed with a seawater sample from the coral reef BR station to determine if the added GBT caused the release of DMSP from the particulate phase into the dissolved phase. This incubation was conducted in the same manner as all other dark incubations, except that in this case subsamples were collected for the measurement of both dissolved and total DMSP ($DMSP_t$).

For each time point, 15 mL subsamples from the acrylate and DMSP incubations were gravity filtered using precombusted, 25 mm diameter GF/F filters into 20 mL scintillation vials using the small-volume drip filtration method outlined in Kiene and Slezak (2006). Filtered samples were microwaved to boiling, bubbled with high-purity nitrogen gas to remove DMS, and acidified with 150 µL of Ultrex HCl (Kinsey and Kieber, 2016). All samples were stored at room temperature in dark for analysis after they were transported back to Syracuse, NY.

Coral symbiont cultures

Non-axenic batch cultures of five coral dinoflagellate symbionts including *Breviolum aenigmaticum*, *Cladocopium* sp., *Durusdinium trenchii*, *Effrenium voratum*, and *Breviolum minutum* were grown at the State University of New York (SUNY), Buffalo Undersea Reef Research Culture Collection. Triplicate cultures were maintained in 30 mL f/2 medium under a 14:10 h light:dark cycle (70–90 µmol quanta m^{-2} s^{-1}, from 34 W fluorescent lights) at 26°C in 50 mL polycarbonate flasks (Bayliss et al., 2019). All cultures were sampled at their approximate exponential growth phase determined by the number of motile cells counted by microscopy.

A 2 mL aliquot of each culture was collected into a 5 mL Qorpak vial followed by immediate addition of 10 µL 50% glutaraldehyde solution (Fisher Scientific) to preserve the sample for cell volume and cell number measurements using a Beckman-Coulter Z2 Particle Counter and Size Analyzer. To collect dissolved samples, 15 mL of culture was gravity filtered through a 25 mm diameter A/E glass fiber filter (Pall) in a Gelman polysulfone filtration tower. For each filtration, the first 5–6 drops were discarded, and the filtrate was then collected in a 20 mL scintillation vial. To collect total samples, 10 mL of unfiltered sample was collected in a 20 mL scintillation vial. Both dissolved and total samples were microwaved until boiling in the SUNY Buffalo lab. After returning to the home laboratory approximately 3 h later, each sample was bubbled using ultrapure helium for 15 min followed by acidification using 150 µL of Ultrex HCl. Samples were stored at room temperature in dark until analyzed.

DMSP, DMSO and acrylate quantification

To measure concentrations of DMSP and DMSO, both compounds were first converted to dimethylsulfide (DMS). To convert DMSP or DMSO to DMS, 200 µL 5 M NaOH or 20% $TiCl_3$, respectively, was added to 1 mL of a standard or seawater sample in a precleaned borosilicate serum vial, which was immediately capped with a Teflon-lined butyl rubber stopper and sealed with an aluminum crimp cap. The DMSP samples

were incubated overnight at room temperature in dark; for the DMSO samples, serum vials were incubated at 55°C in a water bath for 1 h. DMS was analyzed using a cryogenic purge-and-trap system and a Shimadzu GC-14A with a flame photometric detector (Kinsey et al., 2016).

Acrylate concentrations were determined using a pre-column derivatization HPLC method that provided sufficient sensitivity for the analysis of low nM acrylate concentrations in seawater (Tyssebotn et al., 2017). For derivatization, 300 µL thiosalicylic acid (TSA, 20 mM) reagent in MeOH was pipetted into a 5 mL precleaned borosilicate vial containing 3 mL of a standard or seawater sample. Following pH adjustment to 4.0, each vial was tightly screw-capped and incubated at 90°C in a water bath for 6 h. After cooling to room temperature, each derivatized sample was first filtered using a 0.2 µm Nylon syringe filter (Pall) followed by injection of 1 mL into the Shimadzu HPLC system containing a reverse phase Waters HPLC column with UV detection at 257 nm to quantify the acrylate-TSA derivative. The limit of detection of this method is 0.2 nM for a 1 mL injection.

CDOM absorbance

The absorbance spectrum of 0.2 µm-filtered seawater was determined between 240 and 800 nm using a SD 2000 fiber optic spectrophotometer (Ocean Optics) equipped with a 101 cm pathlength capillary cell (World Precision Instruments) precleaned using MeOH and Milli-Q water. Each blank (Milli-Q water) or seawater sample was gently drawn into the capillary cell using a Rainin Rabbit-Plus peristaltic pump. All absorption spectra were baseline corrected by adjusting the absorbance between 630 and 640 nm to zero. The absorbance (A_λ) was converted to an absorption coefficient (a_λ, m^{-1}) using the equation $a_\lambda = 2.303A_\lambda/l$, where l is the cell pathlength determined according to the procedure in Cartisano et al. (2018).

Ancillary measurements

The sea-surface temperature was recorded using a SBE56 sensor (Sea-Bird Scientific) continuously flushed with pumped-in near surface seawater. For total organic carbon (TOC), 30 mL samples of unfiltered seawater were collected in acid-cleaned polycarbonate bottles and stored in the dark at −20°C until analysis. They were analyzed in triplicate with a Shimadzu TOC-LCSV, with Milli-Q water as a blank, potassium hydrogen phthalate as the calibration standard, and deep Sargasso Sea water as the reference. For particulate organic carbon (POC), 500–2000 mL of seawater was filtered through a pre-combusted (450°C, 4 h) 25 mm diameter GF/F glass fiber filter (Whatman), which was stored frozen at −20°C. Prior to analysis, the GF/F filters were thawed in an HCl-saturated atmosphere for 24 h to remove inorganic compounds. The filters were then dried and analyzed using an elemental analyzer (Perkin-Elmer 2400 CHN). For Chlorophyll *a* (Chl *a*), 250 mL seawater was filtered through a 25 mm diameter GF/C glass fiber filter (Whatman) that was subsequently stored frozen at −20°C. The pigments were extracted into 90% acetone at 4°C in the dark for 24 h. The fluorescence of the extracts was measured with a calibrated Turner Designs fluorometer. The abundance of micro-phytoplankton was determined under light microscopy using the Utermöhl technique (Utermöhl, 1958) on 100 mL of sedimented samples fixed with formalin-hexamine to a final concentration of 0.4%. For enumeration of heterotrophic prokaryotes (including bacteria and archaea) and pico- and nano-phytoplankton, samples were fixed with glutaraldehyde (0.5%) and analyzed by flow cytometry (CyFlow Cube 8, Sysmex Partec). For bacterioplankton quantification, samples were stained with SYBRgreen I (∼ 20 µM final concentration) prior to analysis following Gasol and Del Giorgio (2000). For pico- and nano-phytoplankton, forward scatter and red and orange autofluorescence was used to discriminate different populations following Olson et al. (2018). For nitrate, nitrite and phosphate, 10 mL aliquots of unfiltered seawater were collected in 12 mL polypropylene tubes and stored frozen at −20°C. These dissolved inorganic nutrients were quantified by standard, segmented flow analysis with colorimetric detection using a Bran & Luebe autoanalyzer and the procedure outlined in Hansen and Koroleff (1999).

Statistical analyses

Statistics including the Pearson correlation and t-test were performed using SigmaPlot software (version 11.0). Unless otherwise noted, t-tests were performed when data were normally distributed, as determined by the Shapiro–Wilk test. A Mann–Whitney Rank Sum test was used when normality tests failed. Minitab (version 21.2, Minitab LLC) was used to perform Principal Component Analysis (PCA) on a correlation matrix composed of 11 variables and 27 rows of data; an orthogonal regression analysis was used to compare total acrylate ($acrylate_t$) to total DMSP ($DMSP_t$), since measurement error was associated with both parameters. An α level of 0.05 was used for all statistical analyses. Standard deviations were used to report errors, unless otherwise noted.

Results and discussion

Biogeochemical properties along the transect

The daytime temperature in surface waters along the reef-ocean transect was nearly the same throughout the study, averaging 28.8 ±

0.01°C (Table 1). Chl *a* concentrations averaged between 0.18 ± 0.08 and 0.33 ± 0.10 μg L^{-1} among the transect stations, with slightly higher Chl *a* at CH and CO and the lowest Chl *a* observed at the open ocean station (Figure S2; Table 1). A drop in Chl *a* concentration occurred as the water flowed from the fore reef (CO) into the back reef (BR). Similar to prior studies in the Mo'orea coral reef (Nelson et al., 2011; Leichter et al., 2013), nitrate concentrations (and silicate, data not shown) in the coral reef were markedly higher than at the open-ocean sites at stations SO and OO (0.31 ± 0.03 vs 0.06 ± 0.02 μM; Table 1), which may be attributed to the elevated activity of nitrifying bacteria associated with corals (Beman et al., 2007; Wegley et al., 2007). Despite this elevated activity, overall the coral holobiont is expected to be a large sink for nitrate (Glaze et al., 2021). Therefore, there must be other nitrate sources to the coral reef to maintain the relatively high nitrate concentrations we observed. Potential sources include groundwater inputs (Nelson et al., 2015) or sediment resuspension (Erler et al., 2014). Similar trends of lower oceanic concentrations were seen for nitrite and phosphate, but differences were much smaller (Table 1). Nelson et al. (2011) observed a depletion of dissolved organic carbon (DOC) in the Mo'orea coral reef compared to the open ocean over a 4-year time period (68 vs 79 μM DOC). A similar difference was noted in our study, but observed differences (67.8 ± 5.2 in the open ocean vs 75.0 ± 5.7 μM in the coral reef) were not statistically significant ($p > 0.05$). The particulate organic carbon (POC) pool was small relative to DOC, ranging from 3.3 to 4.2 μM throughout the entire transect comprising less than 5% of the total organic carbon signal and with no differences noted between the coral reef and open-ocean sites.

During the main transect study, dinoflagellates and coccolithophores dominated the abundance of micro-phytoplankton, with relatively few diatoms present at the open-ocean stations or in the coral reef. The planktonic assemblage in the coral reef and open-ocean stations exhibited some marked differences, with dinoflagellate and coccolithophore cell numbers in near surface waters nearly double at the open-ocean stations SO and OO (~ 8×10^3 cells L^{-1}) compared to the back reef station (~ 4×10^3 cells L^{-1}). The summed abundances of pico- and nano-eukaryotic phytoplankton were lowest at the farthest open-ocean station OO (2.5×10^6 cells L^{-1}), increased to the highest cell numbers at SO and the fore reef (CO) ($4–5\times10^6$ cells L^{-1}), followed by a decrease to ca. 3×10^6 cells L^{-1} inside the coral reef. A similar yet clearer pattern of decrease into the reef was observed for *Synechococcus* (15×10^6 cells L^{-1} at OO, 50×10^6 cells L^{-1} at SO and CO, 25×10^6 cells L^{-1} at BR) and heterotrophic prokaryote abundances (ca. 0.9×10^9 cells L^{-1} at OO, SO and CO, and 0.5×10^9 cells L^{-1} at BR), but not for *Prochlorococcus* (gradual yet not significant decrease from 90×10^6 cells L^{-1} outside the reef to 70×10^6 cells L^{-1} inside the reef (Figure S2). Depletion of both autotrophic and heterotrophic microbial abundances was previously observed as the water crossed the reef crest into the back reef in this same northern Mo'orean coral reef (Payet et al., 2014), and this was attributed to top down control by coral filter feeding (Patten et al., 2011).

Transects of acrylate and organosulfur concentrations

The range of $acrylate_d$ (0.8–3.9 nM) and $acrylate_t$ concentrations (1.1–5.2 nM) in the transect are small (Figure 2A), and similar to those determined in the Gulf of Mexico in late fall, 0.8–2.1 nM for $acrylate_d$ and 1.4–3.4 nM for $acrylate_t$ (Tyssebotn et al., 2017), but one to three orders of magnitude lower than those previously observed off the coast of China in coastal and open ocean waters across different seasons. Concentrations in Chinese waters ranged from 60–578 nM in Jiaozhou Bay (Wu et al., 2015), 14–353 nM (Liu et al., 2016a) and 4.3–103 nM (Wu et al., 2020) in the Yellow and Bohai Seas, and 10–107 nM in the Changjiang Estuary and East China Sea (Wu et al., 2017). These high $acrylate_d$ concentrations are quite surprising since these waters are characterized by low algal biomass (Chl *a* < 0.5 μg L^{-1}), predominance of low DMSP producers (e.g., diatoms; Liu et al., 2016b), and fast photolysis

TABLE 1 Location of the sampling stations depicted in Figure 1, and the average temperature and concentrations of Chl *a*, nitrate, nitrite, ammonium, phosphate, dissolved organic carbon (DOC), particulate organic carbon (POC) and dissolved organic nitrogen (DON) in seawater samples collected from repeated sampling at each station over a two-week period.

Station	Lat. (°S)	Long. (°W)	Temp. (°C)	Chl *a* (μg L^{-1})	Nitrate	Nitrite	Ammonium	Phosphate (μM)	DOC	POC	DON
CH	17.484	149.839	28.7 (0.1)	0.31 (0.10)	0.30 (0.05)	0.05 (0.01)	0.29 (0.18)	0.16 (0.02)	63.9 (3.7)	4.2 (0.7)	4.2 (0.3)
BR	17.479	149.840	28.8 (0.2)	0.22 (0.06)	0.33 (0.06)	0.05 (0.01)	0.37 (0.12)	0.16 (0.02)	72.9 (8.8)	3.3 (0.3)	4.7 (0.6)
CR	17.477	149.839	28.8 (0.2)	0.25 (0.05)	0.29 (0.06)	0.05 (0.01)	0.29 (0.21)	0.16 (0.01)	66.5 (3.1)	4.0 (1.0)	3.9 (0.2)
CO	17.475	149.839	28.8 (0.2)	0.33 (0.10)	0.17 (0.07)	0.04 (0.01)	0.41 (0.32)	0.14 (0.02)	72.2 (8.5)	3.6 (0.3)	4.1 (1.1)
SO	17.467	149.839	28.8 (0.1)	0.28 (0.02)	0.08 (0.04)	0.05 (0.03)	0.88 (0.32)	0.13 (0.01)	74.5 (6.1)	4.4 (1.0)	4.9 (1.0)
OO	17.457	149.840	28.8 (0.4)	0.18 (0.08)	0.04 (0.01)	0.03 (0.03)	0.48 (0.36)	0.13 (0.02)	75.4 (5.3)	3.4 (0.6)	4.0 (1.2)

Values in parentheses denote the standard deviation (n = 4–5).

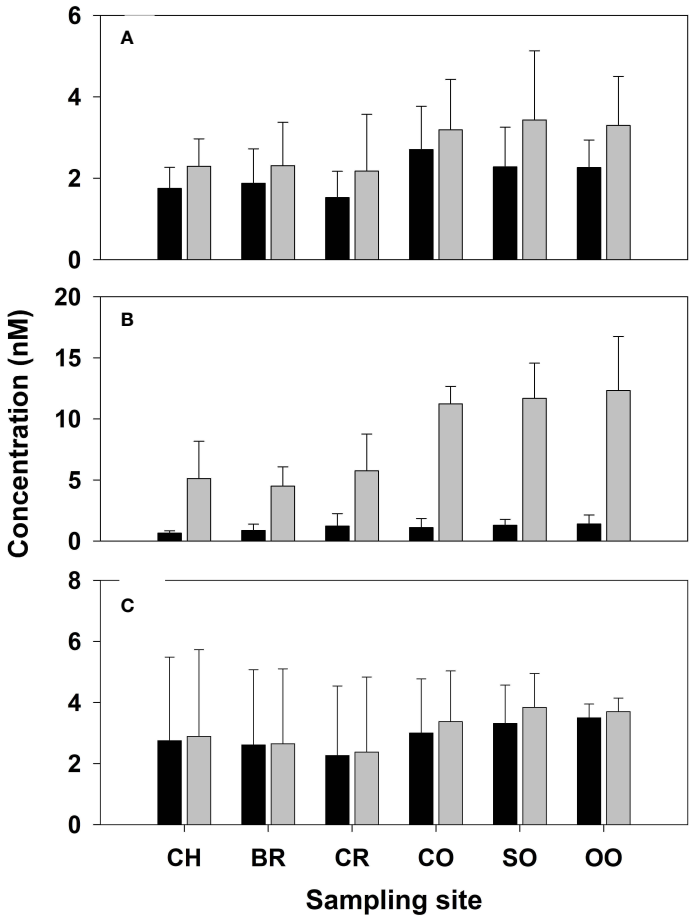

FIGURE 2
Mean dissolved (black-filled bars) and total (grey-filled bars) concentrations of **(A)** acrylate, **(B)** DMSP, and **(C)** DMSO in samples collected from repeated sampling at each sampling station between April 6 and 24, 2018. Error bars denote the standard deviation from the measurement of multiple samples collected over different days at each site (n = 4–5).

and biological consumption rates for $acrylate_d$. Additionally, $acrylate_d$ concentrations in these coastal waters were often substantially greater than its presumptive source DMSP (e.g., Wu et al., 2020). Wu et al. (2017) speculated that anthropogenic sources significantly contributed to the high $acrylate_d$ concentrations observed in their seawater samples, but they supplied no evidence to support this supposition and spatial distributions are inconsistent with an anthropogenic source. The basis for these large differences is not known, however, we speculate that their high acrylate concentrations were due to an artifact associated with co-eluting interferences in the direct HPLC–UV absorption method used to quantify acrylate (non-selective absorption detection at 210 nm).

DMSP concentrations in the Mo'orea coral reef transect study ranged from 0.3–2.8 nM and 2.8–11.1 nM for $DMSP_d$ and $DMSP_t$ (Figure 2B), respectively, slightly lower than $acrylate_d$ and higher than $acrylate_t$. $DMSP_d$ concentrations (1.1 ± 0.7 nM) were comparable to $DMSP_d$ concentrations reported in the literature using the same technique (< 2 nM) to filter samples collected under non-bloom conditions in the Atlantic (Lizotte et al., 2012; Levine et al., 2016), Pacific (Royer et al., 2010), Southern (Kiene et al., 2007), and Arctic Oceans (Motard-Côté et al., 2012). However, when compared to other coral-reef studies, $DMSP_d$ measured in Mo'orea was a factor of 3.5 to 6 lower than mean concentrations at three coral reefs in the Great Barrier Reef (Jones et al., 2007) including Pioneer Bay reef (3.2 nM), Nelly Bay reef (3.7 nM) and One Tree reef (5.5 nM). By comparison, $DMSP_p$ concentrations in the Mo'orea reef (4.2 ± 2.1 nM), determined by subtracting $DMSP_d$ from $DMSP_t$ and propogating the error, were similar to that in Pioneer Bay reef (3.3 nM) and Nelly Bay reef (2.2 nM) but 3.6 times lower than the mean concentration at One Tree reef (15.2 nM). Burdett et al. (2013) only reported $DMSP_t$ concentrations (range 14.7–23.9 nM, mean 19.5 nM) in waters collected along a transect across Suleman reef, Egypt, nearly four-fold higher than the mean $DMSP_t$ concentration in the Mo'orea coral reef (5.1 nM).

Differences between our DMSP results and prior coral-reef studies reflect dissimilarities in reef structure between the Mo'orea reef that was continuously submerged (only the reef crest was occasionally exposed to air) and several prior studies in the Great Barrier Reef where coral were periodically exposed to air and the associated physical stress. Deschaseaux et al. (2014) observed that increases in temperature, reduced salinity, air exposure, and high or low levels of sunlight resulted in greater oxidative stress and enhanced production of DMSP and DMSO in the coral holobiont. Likewise, Raina et al. (2013) determined higher levels of DMSP in thermally stressed *A. millepora* and *A. tenuis*. Higher particulate DMSP concentrations resulting from these physical stresses translate to higher fluxes of DMSP, DMSO (and presumably acrylate) into the dissolved phase. Differences in $DMSP_d$ will also arise from differences in the predominant corals present in the coral reef. In the Great Barrier Reef, *Acropora* sp. is a common reef-building coral (Dietzel et al., 2020) whereas *Pocillopora* sp. is an important coral in Mo'orea (Carlot et al., 2020), and, as will be discussed in the next section, *Acropora pulchra* is a much stronger source of $DMSP_d$ and $acrylate_d$ compared to *Pocillopora* sp. Differences in filtration techniques used to collect dissolved samples may also be at least partially responsible for the difference in $DMSP_d$ concentrations. The Great Barrier Reef samples were filtered using a 0.45-μm filter and peristaltic pump that may have ruptured cells and released DMSP from the particulate phase into dissolved phase. For Mo'orean waters, we collected dissolved samples using a small-volume drip filtration method using a GF/F filter (nominal pore size 0.7 μm), which has been showed to minimize the release of DMSP from algal cells (Kiene and Slezak, 2006).

Although not a main thrust of our study, DMSO concentrations were determined to provide context for the acrylate and DMSP results. In the transect, $DMSO_d$ fell within a wide range between 0.33–6.1 nM, but with no differences noted between the coral-reef stations and the open-ocean stations (Figure 2C). In all our samples, greater than 90% of the DMSO was detected in the dissolved phase (Figure 2C), with very little DMSO present in the particulate pool due to its rapid diffusion out of the cell into the dissolved phase (Spiese et al., 2016). Compared to $DMSP_d$ and DMS (DMS results presented in Masdeu-Navarro et al., 2022), $DMSO_d$ was the main contributor to the dissolved organic sulfur pool averaging nearly 3 nM throughout Mo'orea study. There are several potential sources of $DMSO_d$ in our study area including inputs from the particulate phase (e.g., from DMSO production in planktonic algae, macroalgae, the coral holobiont and subsequent diffusion into the dissolved phase), photochemical oxidation of DMS, or bacterial production from DMS (e.g., trimethylamine monooxygenase activity; Lidbury et al., 2016). These multiple sources, coupled with the chemical stability of DMSO, it's low volatility, and slow microbial consumption (Tyssebotn et al., 2017) likely led to its higher dissolved concentrations compared to dissolved DMS or DMSP, a finding that is consistently observed throughout the world's oceans and in coral reef ecosystems (e.g., Simó et al., 1997; Broadbent and Jones, 2004; del Valle et al., 2007; Kiene et al., 2007; Jones et al., 2007; Asher et al., 2017). Although DMSO was the main dissolved organosulfur compound detected in the Mo'orea coral reef, concentrations were nonetheless lower than found in other oceanic regions including, for example, the Western Mediterranean (Simó et al., 1997), Ross Sea (del Valle et al., 2007), Southern Ocean (Kiene et al., 2007), Gulf of Mexico (Tyssebotn et al., 2017), and Northeast Subarctic Pacific (Asher et al., 2017; Herr et al., 2021). Likewise, $DMSO_d$ concentrations reported here were much lower than $DMSO_d$ concentrations in two Great Barrier Reef studies including Nelly Bay reef (Broadbent and Jones, 2006) and One Tree reef (Jones et al., 2007). In these reefs, $DMSO_d$ ranged (mean) from 5.5–215 nM (17 nM) and 7.7–42 nM (17 nM), respectively. The low background $DMSO_d$ concentrations observed in our study compared to other oceanic regions suggest that production rates were lower and/or microbial consumption rates were faster in the Mo'orea coral reef than previously reported (Tyssebotn et al., 2017).

Acrylate and DMSP concentration data shown in Figure 2 were merged to compare the coral reef (CH, BR, and CR) and the open-ocean sites (SO, and OO), since the mean concentration of each compound was indistinguishable among the different stations in each ecosystem. Data from station CO were not included in the reef versus open ocean comparison due to its close proximity to the reef crest (ca. 150 m) and rapid water exchange with the back reef through the reef crest (ca. 36 min) (Hench et al., 2008; Herdman et al., 2015).

Merged $acrylate_d$ concentrations were 1.7 ± 0.7 nM in the coral reef (n = 15) and 2.3 ± 0.8 nM in the open-ocean sites (n = 8), with no significant difference between these two ecosystems ($p > 0.05$). In contrast, mean $acrylate_p$ concentrations (determined by subtracting $acrylate_d$ from $acrylate_t$ and propagating the error) were lower by a factor of two or more in the coral reef, 0.5 ± 0.5 nM, compared to concentrations at stations SO and OO (1.1 ± 0.7 nM). A large percentage of acrylate, ranging from 50 to 95%, was present in the dissolved phase in all surface waters, consistent with previous culture studies (Tyssebotn, 2015; Kinsey et al., 2016). Dissolved and particulate acrylate and DMSP concentrations reported in this section only include water samples more than a meter away from coral and do not include concentrations in the coral holobiont or in close proximity to the coral; concentrations in these environments are expected to be substantially higher as discussed below (also see Tapiolas et al., 2010; Raina et al., 2013; Tapiolas et al., 2013; Masdeu-Navarro et al., 2022).

Merged $DMSP_d$ concentrations ranged from 0.2–3.0 nM in the coral reef at stations CH, BR, and CR (n = 15) and 0.7–2.1 nM in oceanic waters at stations SO and OO (n = 8), with mean concentrations of 0.9 ± 0.7 nM and 1.3 ± 0.6 nM, respectively. No significant difference was observed between the coral reef

and the open ocean concentrations ($p > 0.05$). Unlike acrylate, $DMSP_d$ represented a small fraction of the total DMSP in surface seawater, generally comprising less than 10% throughout all surface samples. A pronouced reef-ocean difference was observed for $DMSP_p$, with concentrations on average ~2.5 times higher at the oceanic sites (SO and OO) compared to the reef sites (10.7 ± 3.1 nM and 4.2 ± 2.1 nM, respectively). Corresponding Chl *a* concentrations varied over a small range from 0.18–0.33 μg L^{-1} between the two ecosystems (Figure S2; Table 1), resulting in markedly higher $DMSP_p$: Chl *a* ratios (nmol:μg) at the oceanic sites compared to the reef sites (46.4 ± 18.8 vs. 15.2 ± 8.1). A similar pattern albeit with smaller differences between the two environments was observed for $acrylate_p$ concentrations (and ratios to Chl *a*), as discussed in the previous paragraph.

Large differences between coral-reef and open-ocean concentrations of $acrylate_p$ and $DMSP_p$ partly reflect differences in (1) the cell-abundance and composition of the oceanic and reef planktonic communities as previously discussed here (e.g., higher dinoflagellate and coccolithophore cell-number densities in the open-ocean stations) or in Leichter et al. (2013) and (2) top-down control of particulate concentrations by coral feeding on pico- and nano-phytoplankton. Differences may also arise from an upregulation of cellular DMSP production (and corresponding increase in DMSP lyase activity and acrylate production) in the algal community in response to oxidative stress in the oligotrophic open-ocean stations from nutrient limitation (Stefels and van Leeuwe, 1998; Spielmeyer and Pohnert, 2012; Bucciarelli et al., 2013; Kinsey et al., 2016). Nitrogen limitation is known to induce the replacement of N-containing osmolytes (e.g., proline or glycine betaine) by DMSP (Keller et al., 1999; Bucciarelli and Sunda, 2003). Nitrogen limitation has also been suggested to induce DMSP biosynthesis as an antioxidant in response to restricted synthesis of N-containing antioxidants such as ascorbate peroxidase (Sunda et al., 2007). However, even though we observed a large depletion in nitrate in the open ocean samples that were more than eight-fold lower than that in the coral reef (0.06 vs 0.33 μM nitrate, Table 1), inorganic N/P ratios remained low throughout the reef-ocean transect, in the 2.2–7.8 range, indicating pervasive inorganic nitrogen limitation throughout the region. Therefore, inorganic nitrogen stress cannot be invoked as the cause for observed differences in $DMSP_p$ and the $DMSP_p$: Chl *a* ratio along the transect, unless the phytoplankton in the reef relied more than the open-ocean phytoplankton on dissolved organic nitrogen (DON, Table 1) as an additional nitrogen source (e.g., Mulholland and Lee, 2009; Moneta et al., 2014). Consequently, the most likely rationale for the decrease in $DMSP_p$ from the open ocean to the coral reef was due to differences in the algal composition as well as the top-down control of $DMSP_p$ by coral feeding.

A significant positive correlation was found between $acrylate_t$ and $DMSP_t$ in surface waters from both the coral reef ($r = 0.63$, $p < 0.0001$, $n = 44$) and oceanic sites ($r = 0.75$, $p < 0.0001$, $n = 38$; Figure 3), which may be expected since $DMSP_p$ is the presumptive biological precursor of acrylate in seawater. However, the correlation was significantly weaker when only particulate concentrations were considered ($r = 0.37$ for the reef, $p > 0.05$; $r = 0.54$ for the oceanic sites, $p > 0.05$), which is not unexpected because an appreciable proportion of particulate-derived acrylate ends up in the dissolved phase whereas very little DMSP is dissolved. No significant correlation was observed in the coral reef or open-ocean sites between dissolved, particulate or total concentrations of acrylate and DMSO, acrylate and Chl *a*, or DMSP and Chl *a*. Principal component analysis (PCA) was performed to further explore these relationships in our study area (Figure S3). The two principal components accounted for 57.5% of the total variation, and the first axis of PCA showed a strong association between the dissolved or total acrylate and $DMSP_t$ and $DMSO_d$, indicating that these variables were highly correlated. However, PCA analysis also indicated that acrylate, DMSP and DMSO were all negatively aligned with Chl *a*, the nutrients nitrate and phosphate; and acrylate, DMSP and DMSO were all poorly correlated to nitrite and ammonium.

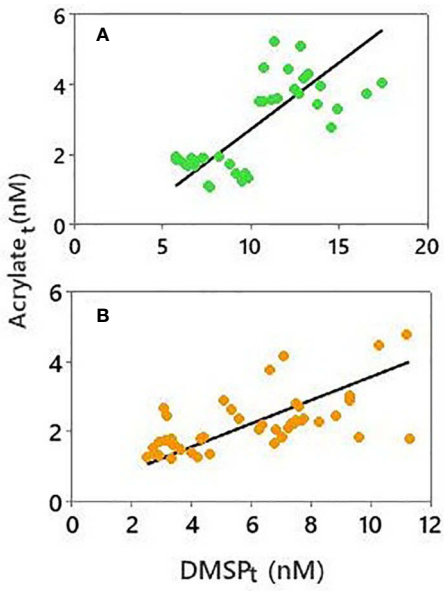

FIGURE 3
Correlation between $acrylate_t$ and $DMSP_t$ in samples collected between 4 and 27 April from the **(A)** oceanic stations (SO and OO) and **(B)** coral reef (CH, BR, CR). Solid lines denote the best-fit from orthogonal regression analysis: **(A)** slope = 0.38 ± 0.06, y-intercept = -1.08 ± 0.60 nM, r = 0.75; **(B)** slope = 0.33 ± 0.06, y-intercept = 0.24 ± 0.41 nM, r = 0.63.

Acrylate and DMSP sources

In the coral reef offshore from Cook's Bay, the main study site, higher $acrylate_d$ concentrations were observed in seawater collected ~0.5 cm away from the coral *A. pulchra* and decomposing seaweed, averaging 18.1 ± 2.9 and 16.5 ± 2.5 nM (Figure 4 and Table S1), respectively, aproximately ten-fold higher than the mean concentration of $acrylate_d$ in surface waters ~2 m from these sources (1.7 ± 0.6 nM). By contrast, no differences were noted in $acrylate_d$ concentrations in close proximity to *Turbinaria ornata* (1.8 ± 0.1 nM) or *Pocillopora* sp. (1.1 ± 0.9 nM) compared to $acrylate_d$ ~2 m from these sources. Although $acrylate_d$ concentrations were low, $acrylate_p$ concentrations (Figure 4 and Table S1) were substantially elevated in waters in close proximity to the macroalgae *T. ornata* (24.9 ± 1.3 nM) or the decomposing seaweed (34.1 ± 4.5 nM) relative to the low $acrylate_p$ concentrations in samples collected from nearby surface seawater (0.5 ± 0.5 nM). Likewise, substantial $DMSP_d$ was detected in close proximity to the coral and macroalgae, averaging 17.6 ± 1.0 nM for the decomposing seaweed, 31.5 ± 0.9 nM for *T. ornata*, and 43.2 ± 0.4 nM for *A. pulchra*, relative to the low average $DMSP_d$ concentration observed in coral reef surface waters (0.9 ± 0.7 nM). A more striking difference was observed for $DMSP_p$, which averaged 21.5 ± 5.3, 186.5 ± 17.3, and 256.5 ± 48.2 nM in waters near *A. pulchra*, *T. ornata*, or the decomposing seaweed (Figure 4 and Table S1), respectively, substantially higher than $DMSP_p$ in coral reef surface waters (4.2 ± 2.1 nM). Together with the large quantities of acrylate and DMSP previously measured in coral tissues and mucus (e.g., Broadbent et al., 2002; Tapiolas et al., 2010; Yost and Mitchelmore, 2010; Raina et al., 2013; Tapiolas et al., 2013; Haydon et al., 2018), it is reasonable to propose that shallow-water coral reefs represent a sizable reservoir of acrylate and organosulfur compounds in the coral-reef ecosystem that may play a disproportionally larger role in regional and global sulfur and carbon cycling than one would predict based on the relatively small areal coverage of coral reefs globally. However, a rigorous evaluation cannot be made here due to the small sample size.

In the Temae Park coral reef study, extremely high concentrations were observed for $acrylate_d$ (65.8 ± 4.2 nM), $DMSP_d$ (80.1 ± 8.9 nM), and $DMSO_d$ (48.4 ± 0.1 nM) in waters a ~0.5 cm away from the coral *A. pulchra*. These concentrations were on average ~30, 40 and 10 times higher than concentrations in waters ~10 cm and several meters away from the coral patch (Figure 5 and Table S2), revealing the large potential of *A. pulchra* as a source of these compounds to the coral reef. The gradients were much smaller for *Pocillopora* sp.; concentrations were 3.2 ± 0.1 nM $acrylate_d$, 6.8 ± 0.1 nM $DMSP_d$, and 4.3 ± 0.4 nM $DMSO_d$ approximately 0.5 cm from the surface of the coral polyps, which were ~3 and 6 times lower away from the *Pocillopora* sp. for $acrylate_d$ and $DMSP_d$ but nearly the same

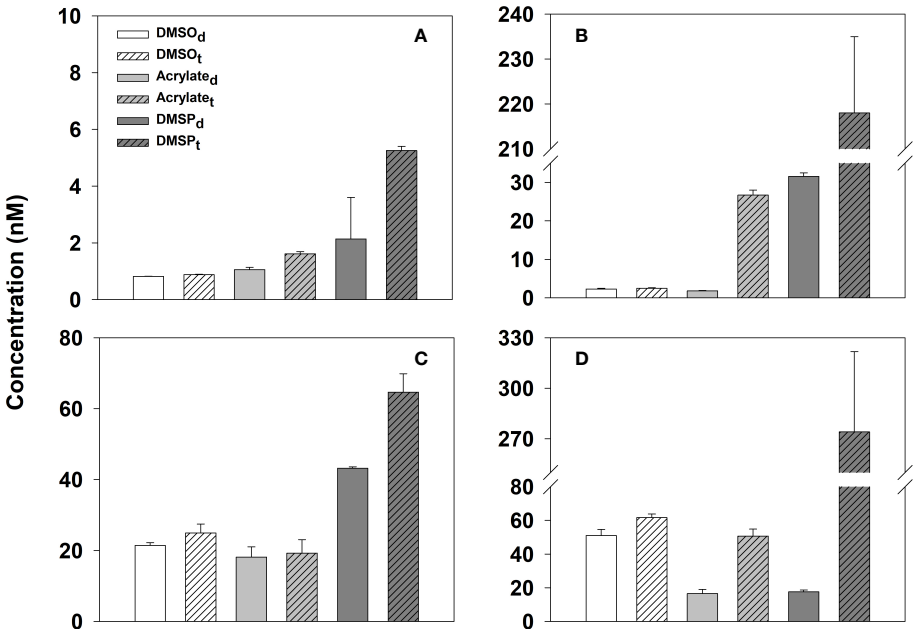

FIGURE 4
Dissolved and total concentrations of acrylate, DMSP and DMSO in samples collected at the CO site between April 15-18 in the vicinity of **(A)** *Pocillopora* sp., **(B)** a brown macroalgae, *Turbinaria ornata*, **(C)** *A. pulchra*, and **(D)** a decomposing seaweed raft. Error bars denote the standard deviation from the measurement of replicate samples. See Table S1 for the data used to generate this figure.

for $DMSO_d$ (Figure 5 and Table S2). Thus, this common coral may be a smaller source of dissolved acrylate and DMSP to the Mo'orea coral reef system compared to *A. pulchra* (also see Figure 4). Overall, *A. pluchara* was a strong source of dissolved acrylate, DMS (DMS data in Masdeu-Navarro et al., 2022), DMSP and DMSO, whereas *Pocillopora* sp. was a weak source for dissolved acrylate and DMSP and not a source of DMSO or DMS (Masdeu-Navarro et al., 2022). The lack of DMS production by *Pocillopora* sp. has been previously observed by Exton et al. (2015) and Lawson et al. (2020), and this likely resulted from low DMSP-lyase activity in *Pocillopora* sp., which would lead to low DMS production rates and low production rates of DMSO from DMS. This in turn likely resulted in no enhancement in $DMSO_d$ concentrations in the vicinity of *Pocillopora* sp. colonies.

Culture-based studies have shown that coral dinoflagellate symbionts contain large quantities of DMSP and DMS (e.g., Broadbent et al., 2002; Steinke et al., 2011; Deschaseaux et al., 2014) and presumably acrylate from the enzymatic lysis of DMSP. However, to date, acrylate concentrations have not been determined in coral algal symbionts although there is a large potential for its production based on the high lyase activity measured in some Symbiodiniaceae (Yost and Mitchelmore, 2009; Caruana and Malin, 2014). In the present study, acrylate and DMSP were detected in non-axenic cultures of five coral dinoflagellate symbionts during exponential growth under nutrient replete conditions (Table 2 and Figure 6). Cellular concentrations of acrylate and DMSP varied among the five species, ranging from 8.6–35.6 mM and 91.9–131.7 mM for acrylate and DMSP, respectively. These cellular acrylate and DMSP concentrations are comparable to those in axenic cultures of other dinoflagellates during early to mid exponential growth under nutrient replete conditions including *Karenia brevis* (2.5–14.5 mM acrylate and 23.0–36.0 mM DMSP; Tyssebotn, 2015) and *Prorocentrum minimum* (3.1–4.2 mM acrylate and 105–160 mM DMSP; Tyssebotn, 2015) or the prymnesiophyte *Phaeocystis antarctica* (3.7–5.2 mM acrylate and 261–275 mM DMSP; Kinsey et al., 2016), and one to two orders of magnitude higher than the diatom *Thalassiosira pseudonana* (0.02–0.25 mM acrylate and 1.8–4.0 mM DMSP; Tyssebotn, 2015). The mM concentrations of acrylate and DMSP observed here for the different coral symbionts suggests coral holobionts produce large quantities of acrylate and DMSP, and are therefore a large potential source of these compounds to the coral-reef ecosystem.

In all coral Symbiodiniaceae cultures, only a small percentage of the total DMSP (< 1%) was detected in dissolved phase, which can be attibuted to its low release from cells and rapid bacterial consumption of $DMSP_d$ in the non-axenic

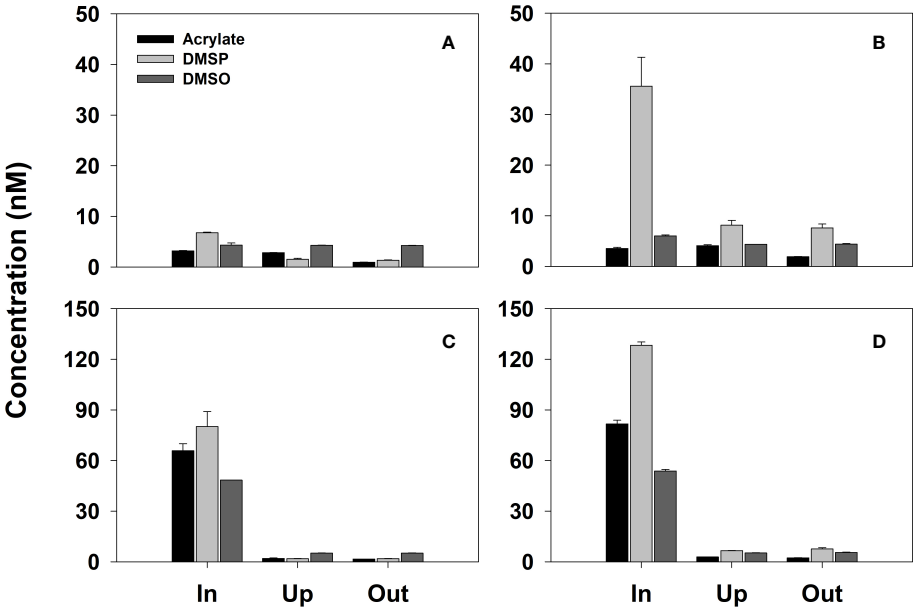

FIGURE 5
Dissolved (panels **A, C**) and total (panels **B, D**) acrylate, DMSP and DMSO in seawater samples collected at different distances from the coral *Pocillopora* sp. (panels **A, B**) and *A pulchra* (panels **C**, **D**) in a coral reef located offshore of Temae Park, Mo'orea at 7:00 am local time, April 23, 2018. x-axis label notation: In, a ~ 0.5 cm away from the tip of several coral polyps, Up, ~ 10 cm away from coral patch, and Out, several meters away from the coral overlying sandy sediment. See Table S2 for the data used to generate this figure.

TABLE 2 Cell size and mean abundance, cell volume (CV), dissolved and cellular concentrations of acrylate and DMSP in five non-axenic, batch cultures of known coral symbionts from the family Symbiodiniaceae.

Species	Cell size	Cell abundance	Cell volume	$Acrylate_d$	$DMSP_d$	$Acrylate_c$	$DMSP_c$
	(μm)	(cells mL^{-1}, $\times 10^6$)	(fL $cell^{-1}$)	(μM)		(mmol L^{-1} CV)	
Breviolum aenigmaticum	7.5	2.35 (0.25)	339 (15)	1.66 (0.54)	0.30 (0.10)	29.6 (10.5)	91.9 (8.6)
Cladocopium sp.	8.8	1.15 (0.16)	399 (27)	0.56 (0.11)	0.16 (0.02)	8.6 (2.5)	118.2 (22.1)
Durusdinium trenchii	9.5	0.82 (0.11)	462 (22)	0.57 (0.22)	0.008 (0.003)	35.6 (4.7)	121.3 (18.6)
Effrenium voratum	11.8	1.71 (0.19)	791 (96)	0.64 (0.17)	0.23 (0.04)	14.6 (3.5)	130.3 (27.9)
Breviolum minutum	6.8	2.10 (0.24)	310 (5)	1.36 (0.18)	0.37 (0.06)	14.7 (1.2)	131.7 (8.0)

Samples were collected for each culture during exponential growth. Values in parentheses denote the standard deviation from triplicate cultures.
The subscripts d and c denote dissolved and cellular, respectively. Cellular concentrations are mmol per liter cell volume.

cultures. Dissolved acrylate concentrations were higher than DMSP, ranging from 3.1 to 13% of the total acrylate; this percentage was significantly less than expected based on results from prior studies under similar growth conditions but with axenic cultures. In these prior studies, which included results from several different dinoflagellate species, from 50-95% of the total acrylate was present in the dissolved phase (Tyssebotn, 2015; Kinsey et al., 2016). The significantly lower percentage of $acrylate_d$ observed in our non-axenic Symbiodiniaceae cultures was likely due to the bacterial consumption of $acrylate_d$ in the culture medium.

Photochemical production of acrylate

Photochemical production of acrylate was consistently observed in the field using freshly collected, 0.2 μm-filtered seawater (Table 3), with no evidence for acrylate photolysis in

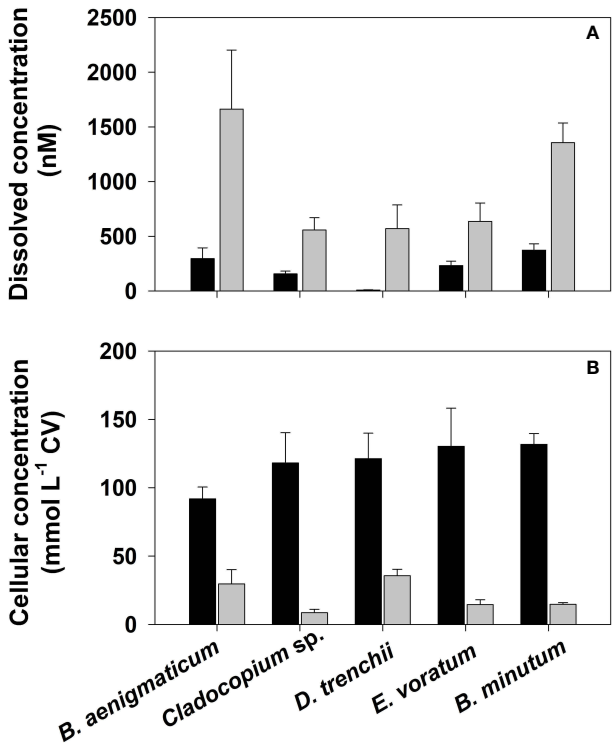

FIGURE 6
(A) Dissolved and **(B)** cell volume (CV) normalized cellular concentrations of acrylate (grey-filled bars) and DMSP (black-filled bars) in non-axenic batch cultures of five dinoflagellate coral symbionts during their exponential growth phase. Error bars represent the standard deviation determined from the analysis of three separate cultures. See Table S3 for culture collection and strain designations.

seawater at ambient concentrations (Xue and Kieber, 2021). To directly compare photochemical production results across different experiments, rates were expressed as a function of the photon exposure (instead of exposure time) between 330 and 380 nm as determined by nitrite actinometry. Photon-based production rates varied by approximately 55%, ranging from 1.6 to 2.9 pM (μmol quanta $cm^{-2})^{-1}$ in the back reef and open-ocean seawater samples (Table 3). Photochemical production rates of acrylate in the coral reef samples at station BR (mean, 2.3 pM (μmol quanta $cm^{-2})^{-1}$) were statistically the same as the oceanic rates at station OO (mean, 2.3 pM (μmol quanta $cm^{-2})^{-1}$) even though the CDOM absorbance coefficient at 330 nm in the back reef samples was on average 79% greater than in the open ocean samples (0.128 vs 0.0715 m^{-1}, respectively). Photochemical production rates would have been expected to be substantially higher in the coral reef if they were correlated to the CDOM absorption. Given that rates were not significantly different between these stations suggests that (1) specific precursors, not correlated to the CDOM absorbance, were responsible for the photochemical production of acrylate in these waters, and (2) these precursors were present at similar concentrations in the coral reef compared to the open ocean samples.

The photochemical production rate of acrylate in the sea-surface microlayer sample collected from the BR station was about a factor of two greater than the mean value in the subsurface samples (4.5 vs 2.3 nM (μmol quanta $cm^{-2})^{-1}$) (Table 3). Higher rates in the microlayer relative to the subsurface samples have been previously reported for the photochemical production of several LMW carbonyl compounds (e.g., by a factor of 1.2–25 for glyoxylic acid). This enhancement may arise from differences in DOM composition or the enrichment of organic matter in the microlayer compared to the underlying seawater (Zhou and Mopper, 1997). Although our microlayer photochemical experiment is not central to our coral reef study, our preliminary finding warrants further investigation given the magnitude of the rate enhancement for acrylate in the sea-surface microlayer.

To compare results obtained here with previous studies, acrylate production rates were also expressed in terms of exposure time assuming 10 h of solar radiation exposure per day (0700–1700). Hourly production rates ranged from 0.033 to 0.051 nM h^{-1}, comparable to that determined for glyoxal and methylglyoxal in Atlantic Ocean surface waters (0.06–0.2 and 0.02–0.07 nM h^{-1}, Zhu and Kieber, 2019) and one order of magnitude lower than the photoproduction rates of other carbonyl compounds including acetaldehyde (0.5 nM h^{-1}) and pyruvate (0.2 nM h^{-1}) in the Sargasso Sea (Mopper et al., 1991). The magnitude of this difference was even greater when compared to the photoproduction rates of acetaldehyde or pyruvate in coastal waters (Mopper and Stahovec, 1986; Kieber et al., 1990; de Bruyn et al., 2011; Takeda et al., 2014). Although hourly production rate comparisons are qualitatively useful to assess differences when light-based rate data are not available, it should be noted that hourly rates are not directly comparable (Kieber et al., 2007). Most published hourly production rates were determined during the summer on sunny days, whereas our acrylate hourly production rates were determined in April on days that were at times quite cloudy with periods of rain. The less than sunny condition was evident in the ratio of the nitrite actinometry to SMARTS clear-sky photon exposure that was significantly less than one, ranging from 0.66 to 0.87 (Xue and Kieber, 2021).

$Acrylate_d$ and $DMSP_d$ biological consumption

The biological consumption of $acrylate_d$ in waters from the Mo'orea back reef (BR) and the open ocean (OO) followed first-order decay kinetics (Figure 7). The slope of the best-fit line from linear regression analysis yielded the net biological consumption

TABLE 3 Acrylate concentration in dark controls (dark, n = 4) and light-exposed quartz tubes (light, n = 4), the temperature for each photochemical experiment (T), initial and final CDOM absorption coefficient at 330 nm (a_{330}), and the photon exposure between 311–333 nm and 330–380 nm determined using nitrate and nitrite actinometry, respectively.

Station	Sampling date 2018	Temperature (°C)[a]	a_{330} (m^{-1})		Photon exposure (μmol cm^{-2})		Acrylate (nM)		Production rate[b]
			Initial	Final	311-333 nm	330-380 nm	Dark	Light	
BR	Apr. 16	29.6	0.139	0.106	54.3 (2.6)	405.5 (13.5)	1.6 (0.29)	2.3 (0.31)	1.6 (0.4)
BR	Apr. 18	28.8	0.117	0.093	39.7 (0.2)	309.4 (5.4)	1.7 (0.53)	2.6 (0.40)	2.9 (0.7)
OO	Apr. 07	29.2	0.075	0.069	28.4 (0.5)	225.2 (7.6)	2.1 (0.20)	2.7 (0.17)	2.3 (0.8)
OO	Apr. 10	29.7	0.068	0.063	76.3 (3.5)	580.7 (21.5)	1.5 (0.34)	3.0 (0.50)	2.3 (0.6)
BR Microlayer	Apr. 18	28.8	0.228	0.164	39.7 (0.2)	309.4 (5.4)	4.2 (0.55)	5.6 (0.41)	4.5 (0.7)

[a]Water bath temperature; the temperature fluctuation in the water bath was < 0.5 °C for each experiment. [b]The production rate was calculated by dividing the acrylate production (light – dark) by the nitrite-based photon exposure. Units for production rate are pM (μmol quanta $cm^{-2})^{-1}$.
The sea-surface microlayer sample was collected from the back reef using a glass plate according to Cunliffe et al. (2013). All seawater samples were gravity filtered through a precleaned 0.2 μm Polycap AS 75 capsule filter (Toole et al., 2003). Values in parentheses denote the standard deviation.

rate constant ($k_{bio,acrylate}$). As shown in Table 4, acrylate$_d$ was rapidly consumed in waters from the back reef with $k_{bio,acrylate}$ ranging from 3.4 to 5.1 d^{-1} with a mean of 4.0 ± 0.7 d^{-1}, nearly six-fold faster than in the open ocean several km offshore from the coral reef (mean 0.7 ± 0.2 d^{-1}, range 0.3–1.1 d^{-1}). Rates were faster in the back reef even though heterotrophic prokaryotes in the coral reef surface waters were approximately 30% less abundant than in the open ocean (4.5×10^5 vs 6.6×10^5 cells mL^{-1}, Table 4). This depletion in heterotrophic prokaryotes in the Mo'orea coral reef agreed with that previously observed in these waters over a four-year period (Nelson et al., 2011). The larger consumption rate constants for acrylate$_d$ in the back reef habitat likely reflected differences in the bacterial community composition in reef waters compared to the open ocean (Leichter et al., 2013; Masdeu-Navarro et al., 2022), as well as differences in bacterial activity. Indeed, bacterial protein synthesis rates approached by bioorthogonal non-canonical amino acid tagging (BONCAT; Leizeaga et al., 2017) were ~ 4 times higher in BR than in OO (Masdeu-Navarro et al., unpublished results), likely because of the availability of nitrate and labile organic matter locally produced by the benthic community, including corals, seaweeds and microorganisms (Silveira et al., 2017). As discussed previously, *A. pulchra* and *T. ornata*, both important components of the Mo'orea reef system (Bulleri et al., 2013; Donovan et al., 2020), were important sources of DMSP and acrylate, which may be representative components of a pool of labile organic compounds to the coral reef.

The rapid consumption of acrylate$_d$ in the Mo'orea coral reef is striking when compared to results in the Gulf of Mexico. Tyssebotn et al. (2017) reported that acrylate$_d$ was consumed in unfiltered Gulf of Mexico water samples, with slow turnover times averaging 1.5 and 11 d at the coastal and open-ocean sites, respectively. These turnover times are 6 and 44 times slower than those observed in the Mo'orea coral reef (Figure 8). Although turnover times were faster, acrylate$_d$ concentrations in the coral reef (1.7 ± 0.7 nM) were not statistically different to concentrations in the Gulf of Mexico (1.5 ± 0.4 nM), indicating that in the coral reef there was a concurrent and rapid input of acrylate into the dissolved phase and fast microbial consumption of acrylate$_d$. In the Gulf of Mexico, inputs and removal rates were slow, and the consumption of acrylate$_d$ only contributed 0.013–0.13% to the bacterial carbon demand, suggesting that the role of acrylate$_d$ was negligible as a substrate for the entire heterotrophic community (Tyssebotn et al., 2017). In the Mo'orea coral reef, acrylate is expected to play a more substantial role in the microbial loop due to its extremely fast consumption and the large production from macroalgae and coral (see section Acrylate and DMSP Sources). Given its rapid turnover, further research is warranted to quantify the significance of acrylate as a substrate to the coral reef heterotrophic community.

The microbial consumption of acrylate$_d$ in the Mo'orea coral reef (mean turnover time 6 h, range 4.7–7.0 h) represents some of the fastest turnover times recorded when compared to the biological consumption of other low molecular weight carbon substrates in seawater. Acrylate turnover times are similar to or faster than some

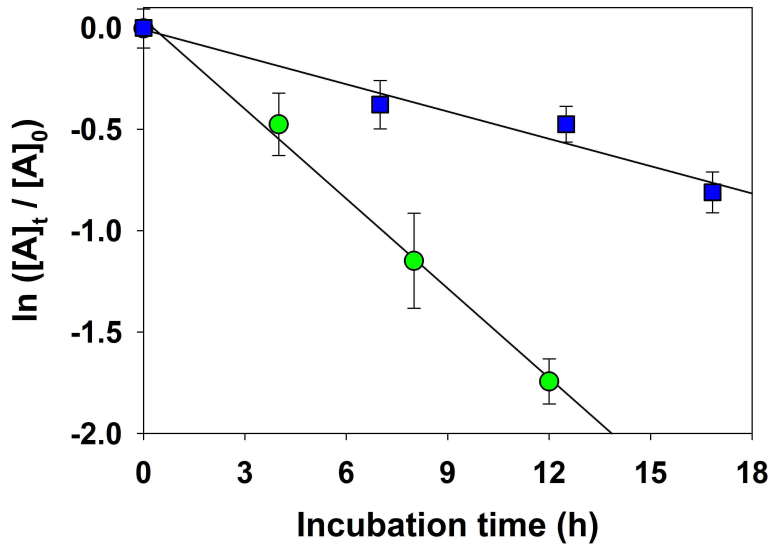

FIGURE 7
First-order kinetic plot for the net biological consumption of acrylate$_d$ in seawater samples collected from the back reef (green circles) and open ocean (blue squares). $[A]_0$ is the initial acrylate concentration and $[A]_t$ is the concentration of a subsample collected during each dark incubation at time t. Error bars denote the standard deviation from triplicate incubations. The biological consumption rate constant, $k_{bio,acrylate}$, was determined by taking the slope of the best-fit line from linear regression analysis.

TABLE 4 Ambient dissolved acrylate and DMSP concentrations, dissolved organic carbon (DOC), particulate organic carbon (POC), and biological rate constants and consumption rates of acrylate and DMSP in the coral-reef BR station and open-ocean OO station collected during diel sampling; local sampling times are reported in the sample column.

Sample	Acrylate$_d$ (nM)	[a]$k_{bio,\ acrylate}$	[b]Acrylate rate	DMSP$_d$ (nM)	[a]$k_{bio,\ DMSP}$	[b]DMSP rate	[c]Bacterial cell number	DOC (μM)	POC (μM)
Reef (BR)									
0400	2.0 (0.19)	3.4 (0.2)	6.8 (0.7)	1.2 (0.06)	5.5 (0.4)	6.4 (0.6)	4.7	76.7	2.8
1000	1.9 (0.12)	4.2 (0.3)	8.0 (0.8)	1.4 (0.05)	8.6 (0.8)	12.1 (1.2)	4.1	66.6	3.2
1600	2.2 (0.14)	4.3 (0.4)	9.4 (1.0)	1.4 (0.03)	8.3 (0.7)	11.6 (1.1)	3.5	64.0	3.5
2200	1.5 (0.16)	3.6 (0.3)	5.4 (0.7)	1.6 (0.05)	7.2 (1.1)	11.8 (1.8)	4.6	67.7	3.4
0400	2.0 (0.06)	3.5 (0.3)	7.0 (0.6)	1.4 (0.07)	7.1 (0.7)	10.2 (1.2)	4.7	68.3	2.8
1000	1.9 (0.11)	5.1 (0.2)	9.7 (0.7)	1.0 (0.05)	8.4 (0.3)	8.5 (0.5)	5.4	72.2	4.4
Mean	1.9 (0.33)	4.0 (0.7)	7.7 (1.9)	1.3 (0.13)	7.5 (1.7)	10.1 (2.7)	4.5 (0.6)	69.3 (4.5)	3.3 (0.6)
Ocean (OO)									
0400	1.4 (0.03)	1.1 (0.1)	1.5 (0.2)	1.3 (0.01)	4.2 (0.4)	5.6 (0.5)	6.6	73.2	2.8
1600	1.6 (0.30)	0.6 (0.1)	0.9 (0.2)	1.8 (0.09)	3.7 (0.6)	6.4 (1.1)	6.5	72.5	3.7
0400	1.7 (0.10)	0.3 (0.1)	0.6 (0.1)	2.1 (0.17)	1.9 (0.6)	3.9 (1.3)	6.4	75.2	3.0
1300	1.1 (0.11)	0.6 (0.1)	0.7 (0.1)	1.6 (0.08)	5.7 (0.3)	9.1 (0.6)	6.8	70.9	3.7
Mean	1.4 (0.33)	0.7 (0.2)	0.9 (0.3)	1.7 (0.21)	3.9 (1.0)	6.2 (1.9)	6.6 (0.2)	73.0 (1.8)	3.3 (0.5)

Values in parentheses denote the standard deviation. Units: [a]biological consumption rate constant (d^{-1}), [b]biological consumption rate (nM d^{-1}), and [c]bacterial cell number ($\times 10^5$ cells mL^{-1}).

of the most labile DOM detected in the oceans, including, for example, dissolved free amino acids (DFAA). Turnover times of DFAA range from 6–48 h in waters off Southern California (Carlucci et al., 1984), 5 and 18 h in high and low productivity Gulf of Mexico waters (Ferguson and Sunda, 1984), and 6.9–144 h (Suttle et al., 1991) and 0.4–7.0 h (Keil and Kirchman, 1999) in Sargasso Sea. Acrylate turnover rates were likely even faster than reported here since we could only determine the net loss of acrylate$_d$ in our study using the non-isotopic technique. If any processes had significantly contributed to the production of acrylate$_d$ during the dark incubation, this would have reduced the observed loss of acrylate and would have reduced the k_{bio} for the biological loss of acrylate. As such, the $k_{bio,acrylate}$ determined from our kinetic approach represent minimum estimates of the true $k_{bio,acrylate}$, which we suspect are faster than reported here. Also, no killed controls were incubated in parallel in our experiments. Therefore, we cannot say unequivocally that acrylate losses were solely due to its biological consumption. However, three lines of evidence suggest biological consumption likely controlled the loss of acrylate in our dark incubations. Acrylate is a highly polar and negatively charged

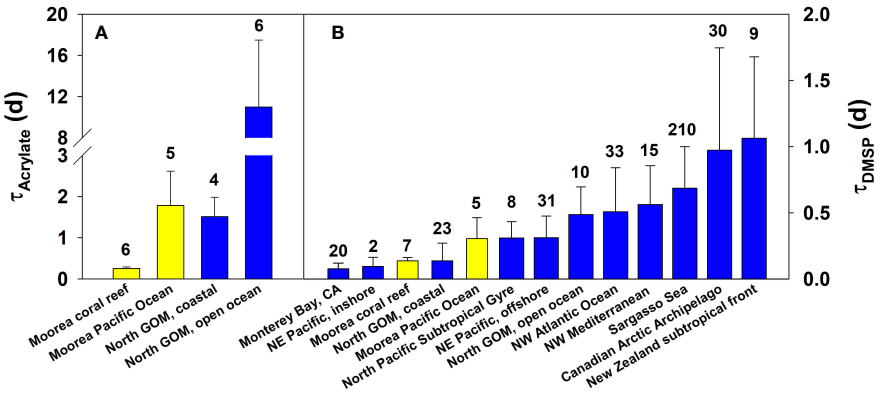

FIGURE 8
Turnover time (τ) of **(A)** acrylate$_d$ and **(B)** DMSP$_d$ from their biological consumption determined in our study (yellow-filled bars) and in previously published studies (blue-filled bars) from different marine environments across different seasons. The value above each bar depicts the number of samples from each study area, which may include multiple studies.

molecule at seawater pH, and therefore is unlikely to be removed from the dissolved phase through complexation or adsorption onto POC; no correlation was observed between POC and $k_{bio,acrylate}$ (Tables 1, 4). Likewise, acrylate is not expected to degrade thermally or by reactions with oxidants, since nM levels of acrylate in seawater were unchanged in filtered dark controls. Finally, biological consumption experiments conducted with unfiltered Gulf of Mexico seawater using nM additions of ^{14}C-labeled acrylate (labeled in the C2 and C3-carbon atoms) demonstrated that acrylate was respired to carbon dioxide and assimilated into macromolecules (Tyssebotn et al., 2017); it is highly unlikely that these products would be produced from abiotic thermal reactions in seawater.

The critical role of DMSP as a substrate for heterotrophic bacteria in seawater is well documented (Kiene et al., 2000; Simó et al., 2009; Buchan et al., 2014); however, its importance as a reduced sulfur and energy source in coral reefs has not been previously studied. Here, using the GBT inhibition technique, we for the first time determined biological consumption rates of $DMSP_d$ in coral-reef waters. The addition of 10 μM GBT in both back-reef and open-ocean waters led to an increase in $DMSP_d$ in the unfiltered samples during the time course of the incubation (Figure 9), resulting from the natural release of particulate DMSP into the seawater through processes such as exudation or grazing while consumption is blocked (Kiene and Gerard, 1995). This assumption is supported by the observation that the time-series decrease in $DMSP_p$ in samples with or without added GBT was the same (t-test, $p > 0.05$, data not shown), suggesting that the external addition of GBT did not artificially cause significant extra release of DMSP from the particulate phase into the dissolved phase in seawater. Therefore, a production rate (R_{prod}) was calculated based on the initial increase of $DMSP_d$ (≤ 3 h) in GBT experiments. In samples receiving no exogenous GBT, $DMSP_d$ decreased rapidly over time (Figure 9) allowing for the calculation of the net loss rate ($R_{loss,net}$). The total loss rate, R_{loss}, was calculated as the sum of R_{prod} and $R_{loss,net}$, and the rate constant for the total loss of $DMSP_d$ ($k_{bio,DMSP}$) was calculated assuming $DMSP_d$ total loss followed first-order kinetics.

Using the GBT approach, we determined that $DMSP_d$ was consumed extremely fast in waters overlying the reef, with $k_{bio,DMSP}$ ranging from 5.5 to 8.6 d^{-1}, nearly twice as fast as the open ocean rates (7.5 ± 1.7 vs 3.9 ± 1.0 d^{-1}, Table 4). Using the rate constants and *in situ* $DMSP_d$ concentrations reported in Table 4, corresponding rates of microbial consumption of $DMSP_d$ in the coral reef and open ocean ranged from 3.9–12 nM d^{-1} (Table 4). If we assume microbial DMS yields from DMSP enzymatic

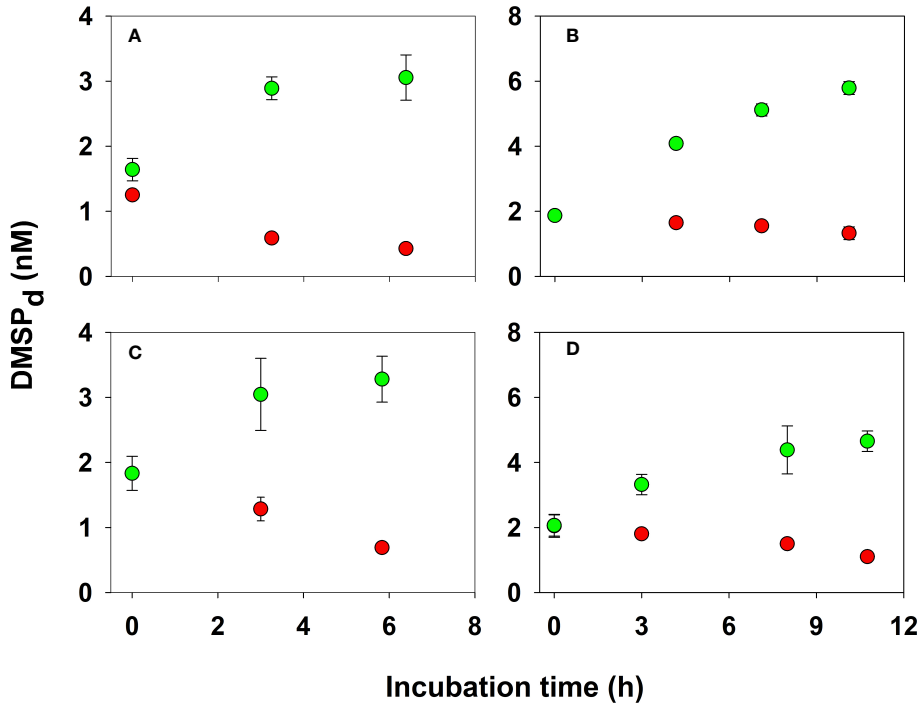

FIGURE 9
Time-course changes in the concentration of $DMSP_d$ in unfiltered seawater from the coral reef (panels **A**, **C**) and open ocean (panels **B**, **D**) incubated in the dark with (green circles) and without (red circles) added GBT (final concentration, 10 μM). Data points denote the mean of triplicate incubations with error bars showing the standard deviation; errors smaller than the symbol are not shown.

cleavage lie between 5–20% (Kiene and Linn, 2000b), then $DMSP_d$ consumption rates would have produced 0.20–2.4 nM DMS daily from this process in the Mo'orea coral reef and adjoining open ocean.

The biological consumption rate constant for $DMSP_d$ was on average nearly twice as fast as that for $acrylate_d$ in the back reef (7.5 ± 1.7 vs 4.0 ± 0.7 d^{-1}), and the difference in k_{bio} (± std dev) was even larger in the open ocean, 3.9 (± 1.0) d^{-1} for $DMSP_d$ and 0.7 (± 0.2) d^{-1} for $acrylate_d$. As shown in Figure 9, our $k_{bio,DMSP}$ in the Mo'orea coral reef was similar to values determined in inshore waters from the northern Gulf of Mexico (Kiene, 1996; Kiene and Linn, 2000a; Pinhassi et al., 2005; Motard-Côté et al., 2016), the northeast Pacific (Royer et al., 2010), and Monterey Bay (Kiene et al., 2019), and nearly 2–10 times faster than the consumption in the open Atlantic (Kiene and Linn, 2000a; Zubkov et al., 2002; Merzouk et al., 2008; Lizotte et al., 2012; Levine et al., 2016; Motard-Côté et al., 2016), Pacific (Merzouk et al., 2006; Royer et al., 2010; del Valle et al., 2012), Mediterranean Sea (Vila-Costa et al., 2008), and polar waters (Luce et al., 2011; Motard-Côté et al., 2012; Lizotte et al., 2017).

Diel study

The first-order rate constant, k_{bio}, for the biological consumption of $acrylate_d$ and $DMSP_d$ varied over the diel cycle in water samples collected from the Mo'orea coral reef and the open ocean (Figure 10). In the back reef (BR), k_{bio} values for both substrates were significantly greater ($p < 0.05$, two-sample t-test) during daylight hours (10:00 and 16:00) compared to nighttime (22:00 and 04:00), exhibiting a clear diel pattern. On average, k_{bio} was 4.5 ± 0.5 d^{-1} for $acrylate_d$ and 8.4 ± 1.1 d^{-1} for $DMSP_d$ in daylight samples, both nearly 30% greater than the mean k_{bio} in night samples. The diel maximum for each substrate was observed in the mid-morning, at 10:00 local time. k_{bio} was 5.1 ± 0.2 d^{-1} for $acrylate_d$ and 8.6 ± 0.8 d^{-1} for $DMSP_d$ at 10:00, both about 1.5-fold faster than the minima observed in the late-night sample at 04:00 on April 12. Even though consumption rate constants varied significantly, dissolved concentrations for both acrylate and DMSP varied very little in the back reef throughout the diel study (Table 4), indicating a tight balance between their production and removal.

In the open-ocean station (OO), several km offshore from the reef, k_{bio} for $acrylate_d$ consumption (0.7 ± 0.2 d^{-1}) was a factor of four or more slower than in the coral reef and no clear diel pattern was observed because of the slower rates and paucity of data (Table 4 and Figure 10). For $DMSP_d$, k_{bio} at the open-ocean site (3.9 ± 1.0 d^{-1}) was two to four times slower compared to the back reef, but, as with acrylate, the diel variation in the open ocean could not be detected due to the lack of sufficient data.

Very few studies have examined diel variations in the biological consumption of specific substrates in the oceans. Carlucci et al. (1984) reported a similar diel pattern for the microbial consumption of DFAA in waters off southern California, as we observed for $acrylate_d$ and $DMSP_d$ in the Mo'orea coral reef; DFAA turnover rates were always faster during daylight hours compared to night-time rates, ranging from 2.5 to 3.7 times and 1.7 to 1.9 times faster during the day compared to night in the spring and fall, respectively. Galí et al. (2013) reported higher rates of microbial consumption of DMS during the day in summer in the Sargasso and the Mediterranean Seas, but no differences in another summer Mediterranean Sea study. The faster biological turnover during the day may be attributed to the higher day time bacterial activity than at night, as has been previously observed from diverse marine locations (Fuhrman et al., 1985; Wheeler et al., 1989; Wikner et al., 1990; Zweifel et al., 1993; Gasol et al., 1998), including coral reef ecosystems (Moriarty et al., 1985; Linley and Koop, 1986), yet not in other studies (Galí et al., 2013). Over the reef flats at Lizard Island, Great Barrier Reef, Moriarty et al. (1985) observed that bacterial growth rates were significantly higher during the day than at night and early morning, and a large increase in growth rates was observed in the late afternoon. Moriarty et al. (1985) proposed that the bacterial growth was mainly stimulated by the release of coral-derived DOM or nutrients carried in the mucus, which also follows a strong diel pattern with maximal rates of release of mucus in the afternoon (Crossland et al., 1980; Wild et al., 2004). In the present study, a pronounced diel variation was observed for $acrylate_d$, $DMSO_d$ and $DMSP_d$ concentrations in waters within ~0.5 cm of the living *A. pulchra* coral host; dissolved concentrations were nearly one order of magnitude higher in samples collected at noon than at midnight (Masdeu-Navarro et al., 2022). This likely resulted from the combination of the expulsion of the algal symbionts during midday hours by the coral polyps (Hoegh-Guldberg et al., 1987) and UVR-induced oxidative stress (Galí et al., 2011). Production and release of organosulfur compounds and acrylate may markedly stimulate the activity of reef-associated bacteria after release into the surrounding water column, which would not be surprising since coral-derived DOC can indeed induce a rapid increase of bacterial abundance and growth rates (Nakajima et al., 2009; Taniguchi et al., 2014; Nakajima et al., 2017; Nakajima et al., 2018).

In contrast to its stimulating effect, studies have also shown that solar radiation, mainly UVR (290–400 nm), can inhibit the growth and activity of bacteria in seawater linked to DNA photodamage (Herndl et al., 1993; Aas et al., 1996; Jeffrey et al., 1996; Alonso-Sáez et al., 2006; Ruiz-González et al., 2013). The faster acrylate and DMSP turnover observed in our daylight samples was most likely a net result between the stimulation

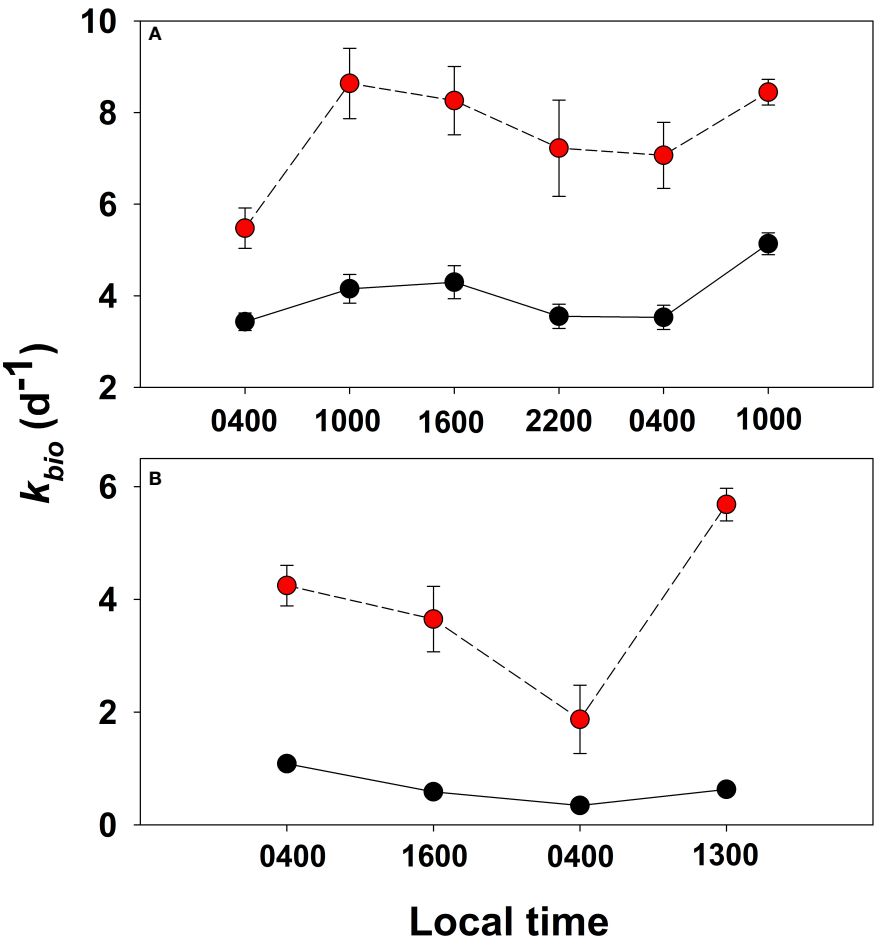

FIGURE 10
First-order rate constant (k_{bio}) for the biological consumption of acrylate$_d$ (black circles) and DMSP$_d$ (red circles) determined from dark incubations of unfiltered seawater collected from the coral reef BR station (panel **A**) and open ocean OO station (panel **B**) during the diel study. Error bars depict the standard deviation from triplicate incubations; errors smaller than the symbol are not shown.

from a larger supply of substrates and inhibition resulting from UVR-induced damage. However, one should note that our diel sampling strategy was to collect samples from a fixed location over time; the disadvantage of this sampling approach is that the same water mass was not followed. Consequently, care should be taken to interpret the diel pattern observed in our study, since it is possible that significantly different microbial populations may have been sampled over the course of the diel study.

Conclusions

Our study provides a novel data set on the distribution and cycling of acrylate and DMSP in a shallow-water coral reef, a severely understudied ecosystem despite its potential for large production and rapid turnover of these compounds in this ecosystem. We observed substantial levels of acrylate and DMSP in waters in the close proximity to important coral and a macroalgae present in the Mo'orea coral reef, as well as in cultures of symbiotic dinoflagellates. Collectively, these results indicate that quantitatively, coral reefs are an important source for acrylate and DMSP. The rapid biological consumption (on a time scale of hours) of dissolved acrylate and DMSP in coral reef waters indicates that these coral-derived substrates serve as efficient carbon, sulfur and energy sources for the growth of reef-associated heterotrophic communities and likely play a critical role in coral reef's ecological network (Figure 11). These new findings call for future studies to quantify the functional role of acrylate and organosulfur compounds in the

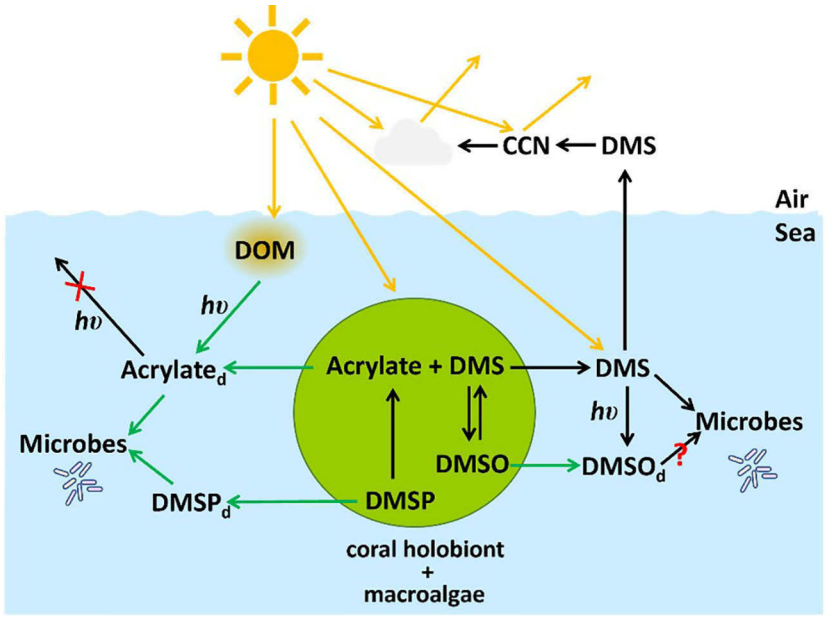

FIGURE 11
A simplified view of the marine organosulfur cycle (1) showing the link between the marine cycle and the atmosphere through DMS and the production of cloud condensation nuclei (CCN), and (2) depicting the main findings of our study highlighted by green arrows. Dissolved acrylate is photochemically produced from the interaction of sunlight (*hυ*) with dissolved organic matter (DOM), and macroalgae and the coral holobiont release acrylate and DMSP into the dissolved phase where they are rapidly consumed by microbes in the Mo'orea coral reef. Acrylate does not photolyze in seawater at ambient concentrations including seawater from the Mo'orea coral reef (Xue and Kieber, 2021) as denoted with a red X. Macroalgae and *A. pulchra* are important sources of dissolved acrylate, DMSP and DMSO. The microbial consumption of DMSO is the presumptive main loss, but this was not confirmed in our study as indicated by the red question mark.

coral holobiont and as microbial substrates in coral-reef environments. Together, this new knowledge will inform the integral role of coral reefs in regional and global carbon and sulfur budgets.

Data availability statement

The datasets used to generate the transect and biological turnover figures in this study are archived in the Biological and Chemical Oceanography-Data Management Office (BCO-DMO) for data management and can be accessed using the following two links doi: 10.26008/1912/bco-dmo.879142.1 and doi: 10.26008/1912/bco-dmo.879158.1. Data presented in this study that are not available from BCO-DMO are provided in Tables S1, S2 in the SM.

Author contributions

DK and LX designed the study. LX analyzed the acrylate, dimethylsulfoniopropionate and dimethylsulfoxide samples, and wrote the initial draft of the manuscript. DK provided review of results and their interpretation and manuscript editing. DK and RS led the field sampling with participation from MM-N, MC-B, PR-R, SG, and CM. MM-N, MC-B, CM and RS analyzed samples for ancillary data. All authors contributed to the article and approved the submitted version.

Funding

This work was supported by funding from the National Science Foundation Chemical Oceanography program (CO–1756907) to DK, from the Spanish Research Agency through the BIOGAPS project (CTM2016-81008-R) to RS, and from EU's Horizon H2020 research and innovation programme through a European Research Council Advanced Grant (ERC-2018-ADG-834162) to RS. The ICM-CSIC holds the 'Severo Ochoa Centre of Excellence' accreditation (CEX2019-000928-S). MC-B, MM-N and PR-R were supported by predoctoral grants from the Spanish government (FPU16-01925 and BES-2017-080048) and "La Caixa" Foundation, respectively. SG was supported by an Australian Government Endeavour Research Fellowship.

Acknowledgments

This work is dedicated to our friend and colleague, Ron Kiene, who's impact on our lives and our work goes well beyond his contributions to the marine-science community, and for that we

are eternally grateful and thankful. We also thank the UC Berkeley Richard Gump Research station staff for logistical support during the field study and Dr. Mary Alice Coffroth at the State University of New York at Buffalo for growing the coral symbiont cultures and sharing lab supplies for sampling. Thanks are also extended to Ms. Liang Chen in Dr. Kieber's laboratory for measuring cell numbers and cell volumes in culture samples, and to Dr. Kristin Bergauer for sharing unpublished BONCAT measurements of bacterial production obtained during our field study.

Conflict of interest

The authors declare that the research was conducted in the absence of any commercial or financial relationships that could be construed as a potential conflict of interest.

Publisher's note

Supplementary material

The Supplementary Material for this article can be found online at: https://www.frontiersin.org/articles/10.3389/fmars.2022.911522/full#supplementary-material

References

Aas, P., Lyons, M., Pledger, R., Mitchell, D. L., and Jeffrey, W. H. (1996). Inhibition of bacterial activities by solar radiation in nearshore waters and the gulf of Mexico. *Aquat. Microb. Ecol.* 11, 229–238. doi: 10.3354/ame011229

Adjeroud, M. (1997). Factors influencing spatial patterns on coral reefs around mo'orea, French Polynesia. *Mar. Ecol. Prog. Ser.* 159, 105–119. doi: 10.3354/meps159105

Alonso-Sáez, L., Gasol, J. M., Lefort, T., Hofer, J., and Sommaruga, R. (2006). Effect of natural sunlight on bacterial activity and differential sensitivity of natural bacterioplankton groups in northwestern Mediterranean coastal waters. *Appl. Environ. Microbiol.* 72, 5806–5813. doi: 10.1128/AEM.00597-06

Asher, E., Dacey, J. W., Ianson, D., Peña, A., and Tortell, P. D. (2017). Concentrations and cycling of DMS, DMSP, and DMSO in coastal and offshore waters of the subarctic pacific during summer 2010-2011. *J. Geophys. Res. C.* 122, 3269–3286. doi: 10.1002/2016JC012465

Bayliss, S. L. J., Scott, Z. R., Coffroth, M. A., and terHorst, C. P. (2019). Genetic variation in *Breviolum antillogorgium*, a coral reef symbiont, in response to temperature and nutrients. *Ecol. Evol.* 9, 2803–2813. doi: 10.1002/ece3.4959

Beman, J. M., Roberts, K. J., Wegley, L., Rohwer, F., and Francis, C. A. (2007). Distribution and diversity of archaeal ammonia monooxygenase genes associated with corals. *Appl. Environ. Microbiol.* 73, 5642–5647. doi: 10.1128/AEM.00461-07

Broadbent, A. D., and Jones, G. B. (2004). DMS and DMSP in mucus ropes, coral mucus, surface films and sediment pore water from coral reefs in the great barrier reef. *Mar. Freshw. Res.* 55, 849–855. doi: 10.1071/MF04114

Broadbent, A., and Jones, G. (2006). Seasonal and diurnal cycles of dimethylsulfide, dimethylsulfoniopropionate and dimethylsulfoxide at one tree reef lagoon. *Environ. Chem.* 3, 260–267. doi: 10.1071/EN06011

Broadbent, A. D., Jones, G. B., and Jones, R. J. (2002). DMSP in corals and benthic algae from the great barrier reef. *Estuar. Coast. Shelf Sci.* 55, 547–555. doi: 10.1006/ecss.2002.1021

Bucciarelli, E., Ridame, C., Sunda, W. G., Dimier-Hugueney, C., Cheize, M., and Belviso, S. (2013). Increased intracellular concentrations of DMSP and DMSO in iron-limited oceanic phytoplankton *Thalassiosira oceanica* and *Trichodesmium erythraeum*. *Limnol. Oceanogr.* 58, 1667–1679. doi: 10.4319/lo.2013.58.5.1667

Bucciarelli, E., and Sunda, W. G. (2003). Influence of CO_2, nitrate, phosphate, and silicate limitation on intracellular dimethylsulfoniopropionate in batch cultures of the coastal diatom *Thalassiosira pseudonana*. *Limnol. Oceanogr.* 48, 2256–2265. doi: 10.4319/lo.2003.48.6.2256

Buchan, A., LeCleir, G. R., Gulvik, C. A., and González, J. M. (2014). Master recyclers: Features and functions of bacteria associated with phytoplankton blooms. *Nat. Rev. Microbiol.* 12, 686–698. doi: 10.1038/nrmicro3326

Bulleri, F., Couraudon-Réale, M., Lison de Loma, T., and Claudet, J. (2013). Variability in the effects of macroalgae on the survival and growth of corals: The consumer connection. *PloS One* 8, e79712. doi: 10.1371/journal.pone.0079712

Burdett, H. L., Aloisio, E., Calosi, P., Findlay, H. S., Widdicombe, S., Hatton, A. D., et al. (2012). The effect of chronic and acute low pH on the intracellular DMSP production and epithelial cell morphology of red coralline algae. *Mar. Biol. Res.* 8, 756–763. doi: 10.1080/17451000.2012.676189

Burdett, H. L., Donohue, P. J. C., Hatton, A. D., Alwany, M. A., and Kamenos, N. A. (2013). Spatiotemporal variability of dimethylsulphoniopropionate on a fringing coral reef: The role of reefal carbonate chemistry and environmental variability. *PLoS One* 8, e64651. doi: 10.1371/journal.pone.0064651

Carlot, J., Rovère, A., Casella, E., Harris, D., Grellet-Muñoz, C., Chancerelle, Y., et al. (2020). Community composition predicts photogrammetry-based structural complexity on coral reefs. *Coral Reefs* 39, 967–975. doi: 10.1007/s00338-020-01916-8

Carlucci, A. F., Craven, D. B., and Henrichs, S. M. (1984). Diel production and microheterotrophic utilization of dissolved free amino acids in waters off southern California. *Appl. Environ. Microbiol.* 48, 165–170. doi: 10.1128/AEM.48.1.165-170.1984

Cartisano, C. M., Del Vecchio, R., and Blough, N. V. (2018). A calibration/validation protocol for long/multi-pathlength capillary waveguide spectrometers. *Limnol. Oceanogr.: Methods* 16, 773–786. doi: 10.1002/lom3.10282

Caruana, M. N., and Malin, G. (2014). The variability in DMSP content and DMSP lyase activity in marine dinoflagellates. *Prog. Oceanogr.* 120, 410–424. doi: 10.1016/j.pocean.2013.10.014

Charlson, R. J., Lovelock, J. E., Andreae, M. O., and Warren, S. G. (1987). Oceanic phytoplankton, atmospheric sulfur, cloud albedo and climate. *Nature* 326, 655–661. doi: 10.1038/326655a0

Crossland, C. J., Barnes, D. J., and Borowitzka, M. A. (1980). Diurnal lipid and mucus production in the staghorn coral. *Acropora acuminata*. *Mar. Biol.* 60, 81–90. doi: 10.1007/BF00389151

Cunliffe, M., Engel, A., Frka, S., Gašparović, B., Guitart, C., Murrell, J. C., et al. (2013). Sea Surface microlayers: A unified physicochemical and biological perspective of the air-ocean interface. *Prog. Oceanogr.* 109, 104–116. doi: 10.1016/j.pocean.2012.08.004

Curson, A. R. J., Liu, J., Bermejo Martínez, A., Green, R. T., Chan, Y., Carrión, O., et al. (2017). Dimethylsulfoniopropionate biosynthesis in marine bacteria and identification of the key gene in this process. *Nat. Microbiol.* 2, 1–9. doi: 10.1038/nmicrobiol.2017.9

de Bruyn, W. J., Clark, C. D., Pagel, L., and Takehara, C. (2011). Photochemical production of formaldehyde, acetaldehyde and acetone from chromophoric dissolved organic matter in coastal waters. *J. Photochem. Photobiol. A Chem.* 226, 16–22. doi: 10.1016/j.photochem.2011.10.002

del Valle, D. A., Kieber, D. J., John, B., and Kiene, R. P. (2007). Light-stimulated production of dissolved DMSO by a particle-associated process in the Ross Sea, Antarctica. *Limnol. Oceanogr.* 52, 2456–2466. doi: 10.4319/lo.2007.52.6.2456

del Valle, D. A., Kiene, R. P., and Karl, D. M. (2012). Effect of visible light on dimethylsulfoniopropionate assimilation and conversion to dimethylsulfide in the north pacific subtropical gyre. *Aquat. Microb. Ecol.* 66, 47–62. doi: 10.3354/ame01557

Deschaseaux, E. S. M., Jones, G. B., Deseo, M. A., Shepherd, K. M., Kiene, R. P., Swan, H. B., et al. (2014). Effects of environmental factors on dimethylated sulfur compounds and their potential role in the antioxidant system of the coral holobiont. *Limnol. Oceanogr.* 59, 758–768. doi: 10.4319/lo.2014.59.3.0758

Dietzel, A., Bode, M., Connolly, S. R., and Hughes, T. P. (2020). Long-term shifts in the colony size structure of coral populations along the great barrier reef. *Proc. R. Soc B.* 287, 20201432. doi: 10.1098/rspb.2020.1432

Donovan, M. K., Adam, T. C., Shantz, A. A., Speare, K. E., Munsterman, K. S., Rice, M. M., et al. (2020). Nitrogen pollution interacts with heat stress to increase coral bleaching across the seascape. *Proc. Nat. Acad. Sci.* 117, 5351–5357. doi: 10.1073/pnas.1915395117

Drew, E. A. (1972). The biology and physiology of algal-invertebrate symbiosis. II. the density of algal cells in a number of hermatypic hard corals and alcyonarians from various depths. *J. Exp. Mar. Biol. Ecol.* 9, 71–75. doi: 10.1016/0022-0981(72)90008-1

Erler, D. V., Santos, I. R., and Eyre, B. D. (2014). Inorganic nitrogen transformations within permeable carbonate sands. *Cont. Shelf Res.* 77, 69–80. doi: 10.1016/j.csr.2014.02.002

Evans, C., Kadner, S. V., Darroch, L. J., Wilson, W. H., Liss, P. S., and Malin, G. (2007). The relative significance of viral lysis and microzooplankton grazing as pathways of dimethylsulfoniopropionate (DMSP) cleavage: An *Emiliania huxleyi* culture study. *Limnol. Oceanogr.* 52, 1036–1045. doi: 10.4319/lo.2007.52.3.1036

Evans, C., Malin, G., Wilson, W. H., and Liss, P. S. (2006). Infectious titres of *Emiliania huxleyi* virus 86 are reduced by exposure to millimolar dimethylsulfide and acrylic acid. *Limnol. Oceanogr.* 51, 2468–2471. doi: 10.4319/lo.2006.51.5.2468

Exton, D. A., McGenity, T. J., Steinke, M., Smith, D. J., and Suggett, D. J. (2015). Uncovering the volatile nature of tropical coastal marine ecosystems in a changing world. *Glob. Change Biol.* 21, 1383–1394. doi: 10.1111/gcb.12764

Ferguson, R. L., and Sunda, W. G. (1984). Utilization of amino acids by planktonic marine bacteria: Importance of clean technique and low substrate additions. *Limnol. Oceanogr.* 29, 258–274. doi: 10.4319/lo.1984.29.2.0258

Fuhrman, J. A., Eppley, R. W., Hagström, Å., and Azam, F. (1985). Diel variations in bacterioplankton, phytoplankton, and related parameters in the southern California bight. *Mar. Ecol. Prog. Ser.* 27, 9–20. doi: 10.3354/meps027009

Galí, M., Saló, V., Almeda, R., Calbet, A., and Simó, R. (2011). Stimulation of gross dimethylsulfide (DMS) production by solar radiation. *Geophys. Res. Lett.* 38, L15612. doi: 10.1029/2011GL048051

Galí, M., Simó, R., Vila-Costa, M., Ruiz-González, C., Gasol, J. M., and Matrai, P. (2013). Diel patterns of oceanic dimethylsufide (DMS) cycling: Microbial and physical drivers. *Global Biogeochem. Cycles* 27, 1–17. doi: 10.1002/gbc.20047

Gardner, S. G., Nielsen, D. A., Laczka, O., Shimmon, R., Beltran, V. H., Ralph, P. J., et al. (2016). Dimethylsulfoniopropionate, superoxide dismutase and glutathione as stress response indicators in three corals under short-term hyposalinity stress. *Proc. R. Soc B* 283, 20152418. doi: 10.1098/rspb.2015.2418

Gardner, S. G., Raina, J.-B., Nitschke, M. R., Nielsen, D. A., Stat, M., Motti, C. A., et al. (2017). A multi-trait systems approach reveals a response cascade to bleaching in corals. *BMC Biol.* 15, 117. doi: 10.1186/s12915-017-0459-2

Gasol, J. M., and Del Giorgio, P. A. (2000). Using flow cytometry for counting natural planktonic bacteria and understanding the structure of planktonic bacterial communities. *Sci. Mar.* 64, 197–224. doi: 10.3989/scimar.2000.64n2197

Gasol, J. M., Doval, M. D., Pinhassi, J., Calderón-Paz, J. I., Guixa-Boixareu, N., Vaqué, D., et al. (1998). Diel variations in bacterial heterotrophic activity and growth in the northwest Mediterranean Sea. *Mar. Ecol. Prog. Ser.* 164, 107–124. doi: 10.3354/meps164107

Glaze, T. D., Erler, D. V., and Siljanen, H. M. P. (2021). Microbially facilitated nitrogen cycling in tropical corals. *ISME J.* 16, 68–77. doi: 10.1038/s41396-021-01038-1

Guibert, I., Bourdreux, F., Bonnard, I., Pochon, X., Dubousquet, V., Raharivelomanana, P., et al. (2020). Dimethylsulfoniopropionate concentration in coral reef invertebrates varies according to species assemblages. *Sci. Rep.* 10, 9922. doi: 10.1038/s41598-020-66290-5

Hansen, H. P., and Koroleff, F. (1999). "Determination of nutrients," in *Methods of seawater analysis*. Eds. K. Grasshoff, K. Kremling and M. Ehrhardt(WILEY-VCH Verlag GmbH), 159–228. doi: 10.1002/9783527613984.ch10

Haydon, T. D., Seymour, J. R., and Suggett, D. J. (2018). Soft corals are significant DMSP producers in tropical and temperate reefs. *Mar. Biol.* 165, 109. doi: 10.1007/s00227-018-3367-2

Hench, J. L., Leichter, J. J., and Monismith, S. G. (2008). Episodic circulation and exchange in a wave-driven coral reef and lagoon system. *Limnol. Oceanogr.* 53, 2681–2694. doi: 10.4319/lo.2008.53.6.2681

Herdman, L. M. M., Hench, J. L., and Monismith, S. G. (2015). Heat balances and thermally driven lagoon-ocean exchanges on a tropical coral reef system (Moorea, French Polynesia). *J. Geophys. Res. C.* 120, 1233–1252. doi: 10.1002/2014JC010145

Herndl, G. J., Müller-Niklas, G., and Frick, J. (1993). Major role of ultraviolet-b in controlling bacterioplankton growth in the surface layer of the ocean. *Nature* 361, 717–719. doi: 10.1038/361717a0

Herr, A. E., Dacey, J. W. H., Kiene, R. P., McCulloch, R. D., Schuback, N., and Tortell, P. D. (2021). Potential roles of dimethylsulfoxide in regional sulfur cycling and phytoplankton physiological ecology in the NE subarctic pacific. *Limnol. Oceanogr.* 66, 76–94. doi: 10.1002/lno.11589

Hill, R. W., Dacey, J. W. H., and Edward, A. (2000). Dimethylsulfoniopropionate in giant clams (Tridacnidae). *Biol. Bull.* 199, 108–115. doi: 10.2307/1542870

Hill, R. W., Dacey, J. W. H., and Krupp, D. A. (1995). Dimethylsulfoniopropionate in reef corals. *Bull. Mar. Sci.* 57, 489–494.

Hoegh-Guldberg, O. (1999). Climate change, coral bleaching and the future of the world's coral reefs. *Mar. Freshw. Res.* 50, 839–866. doi: 10.1071/MF99078

Hoegh-Guldberg, O., McCloskey, L. R., and Muscatine, L. (1987). Expulsion of zooxanthellae by symbiotic cnidarians from the red Sea. *Coral Reefs* 5, 201–204. doi: 10.1007/BF00300964

Jackson, R. L., Gabric, A. J., Woodhouse, M. T., Swan, H. B., Jones, G. B., Cropp, R. A., et al. (2020). Coral reef emissions of atmospheric dimethylsulfide and the influence on marine aerosols in the southern great barrier reef, Australia. *J. Geophys. Res. D.* 125, e2019JD031837. doi: 10.1029/2019JD031837

Jankowski, J. J., Kieber, D. J., and Mopper, K. (1999). Nitrate and nitrite ultraviolet actinometers. *Photochem. Photobiol.* 70, 319–328. doi: 10.1111/j.1751-1097.1999.tb08143.x

Jankowski, J. J., Kieber, D. J., Mopper, K., and Neale, P. J. (2000). Development and intercalibration of ultraviolet solar actinometers. *Photochem. Photobiol.* 71, 431–440. doi: 10.1562/0031-8655(2000)0710431DAIOUS2.0.CO2

Jeffrey, W. H., Pledger, R. J., Aas, P., Hager, S., Coffin, R. B., Von Haven, R., et al. (1996). Diel and depth profiles of DNA photodamage in bacterioplankton exposed to ambient solar ultraviolet radiation. *Mar. Ecol. Prog. Ser.* 137, 283–291. doi: 10.3354/meps137283

Jones, G., Curran, M., Broadbent, A., King, S., Fischer, E., and Jones, R. (2007). Factors affecting the cycling of dimethylsulfide and dimethylsulfoniopropionate in coral reef waters of the great barrier reef. *Environ. Chem.* 4, 310–322. doi: 10.1071/EN06065

Jones, G., Curran, M., Deschaseaux, E., Omori, Y., Tanimoto, H., Swan, H., et al. (2018). The flux and emission of dimethylsulfide from the great barrier reef region and potential influence on the climate of NE Australia. *J. Geophys. Res. D.* 123, 13,835–13,856. doi: 10.1029/2018JD029210

Keil, R. G., and Kirchman, D. L. (1999). Utilization of dissolved protein and amino acids in the northern Sargasso Sea. *Aquat. Microb. Ecol.* 18, 293–300. doi: 10.3354/ame018293

Keller, M. D. (1989). Dimethyl sulfide production and marine phytoplankton: The importance of species composition and cell size. *Biol. Oceanogr.* 6, 375–382. doi: 10.1080/01965581.1988.10749540

Keller, M. D., Kiene, R. P., Matrai, P. A., and Bellows, W. K. (1999). Production of glycine betaine and dimethylsulfoniopropionate in marine phytoplankton. II. n-limited chemostat cultures. *Mar. Biol.* 135, 249–257. doi: 10.1007/s002270050622

Kerrison, P., Suggett, D. J., Hepburn, L. J., and Steinke, M. (2012). Effect of elevated pCO_2 on the production of dimethylsulphoniopropionate (DMSP) and dimethylsulphide (DMS) in two species of ulva (Chlorophyceae). *Biogeochemistry* 110, 5–16. doi: 10.1007/s10533-012-9707-2

Kieber, D. J., Toole, D. A., Jankowski, J. J., Kiene, R. P., Westby, G. R., del Valle, D. A., et al. (2007). Chemical "light meters" for photochemical and photobiological studies. *Aquat. Sci.* 69, 360–376. doi: 10.1007/s00027-007-0895-0

Kieber, D. J., Yocis, B. H., and Mopper, K. (1997). Free-floating drifter for photochemical studies in the water column. *Limnol. Oceanogr.* 42, 1829–1833. doi: 10.4319/lo.1997.42.8.1829

Kieber, R. J., Zhou, X., and Mopper, K. (1990). Formation of carbonyl compounds from UV-induced photodegradation of humic substances in natural waters: Fate of riverine carbon in the sea. *Limnol. Oceanogr.* 35, 1503–1515. doi: 10.4319/lo.1990.35.7.1503

Kiene, R. P. (1996). "Turnover of dissolved DMSP in estuarine and shelf waters of the northern gulf of Mexico," in *Biological and environmental chemistry of DMSP and related sulfonium compounds*. Eds. R. P. Kiene, P. T. Visscher, M. D. Keller and G. O. Kirst (Plenum Press, Boston, MA), 337–349. doi: 10.1007/978-1-4613-0377-0_29

Kiene, R. P., and Gerard, G. (1995). Evaluation of glycine betaine as an inhibitor of dissolved dimethylsulfoniopropionate degradation in coastal waters. *Mar. Ecol. Prog. Ser.* 128, 121–131. doi: 10.3354/meps128121

Kiene, R. P., Kieber, D. J., Slezak, D., Toole, D. A., del Valle, D. A., Bisgrove, J., et al. (2007). Distribution and cycling of dimethylsulfide, dimethylsulfoniopropionate, and dimethylsulfoxide during spring and early summer in the southern ocean south of new Zealand. *Aquat. Sci.* 69, 305–319. doi: 10.1007/s00027-007-0892-3

Kiene, R. P., and Linn, L. J. (2000a). Distribution and turnover of dissolved DMSP and its relationship with bacterial production and dimethylsulfide in the gulf of Mexico. *Limnol. Oceanogr.* 45, 849–861. doi: 10.4319/lo.2000.45.4.0849

Kiene, R. P., and Linn, L. J. (2000b). The fate of dissolved dimethylsulfoniopropionate (DMSP) in seawater: Tracer studies using ^{35}S-DMSP. *Geochim. Cosmochim. Acta* 64, 2797–2810. doi: 10.1016/S0016-7037(00)00399-9

Kiene, R. P., Linn, L. J., and Bruton, J. A. (2000). New and important roles for DMSP in marine microbial communities. *J. Sea Res.* 43, 209–224. doi: 10.1016/S1385-1101(00)00023-X

Kiene, R. P., Nowinski, B., Esson, K., Preston, C., Marin, R., Birch, J., et al. (2019). Unprecedented DMSP concentrations in a massive dinoflagellate bloom in Monterey bay, CA. *Geophys. Res. Lett.* 46, 1–10. doi: 10.1029/2019GL085496

Kiene, R. P., and Slezak, D. (2006). Low dissolved DMSP concentrations in seawater revealed by small-volume gravity filtration and dialysis sampling. *Limnol. Oceanogr. Met.* 4, 80–95. doi: 10.4319/lom.2006.4.80

Kinsey, J. D., and Kieber, D. J. (2016). Microwave preservation method for DMSP, DMSO, and acrylate in unfiltered seawater and phytoplankton culture samples. *Limnol. oceanogr. Methods* 14, 196–209. doi: 10.1002/lom3.10081

Kinsey, J. D., Kieber, D. J., and Neale, P. J. (2016). Effects of iron limitation and UV radiation on *Phaeocystis antarctica* growth and DMSP, DMSO, and acrylate concentrations. *Environ. Chem.* 13, 195–211. doi: 10.1071/EN14275

Lawson, C. A., Seymour, J. R., Possell, M., Suggett, D. J., and Raina, J.-B. (2020). The volatilomes of symbiodiniaceae-associated bacteria are influenced by chemicals derived from their algal partner. *Front. Mar. Sci.* 7. doi: 10.3389/fmars.2020.00106

Leichter, J. J., Alldredge, A. L., Bernardi, G., Brooks, A. J., Carlson, C. A., Carpenter, R. C., et al. (2013). Biological and physical interactions on a tropical island coral reef: Transport and retention processes on moorea, French Polynesia. *Oceanography* 26, 52–63. doi: 10.5670/oceanog.2013.45

Leizeaga, A., Estrany, M., Forn, I., and Sebastián, M. (2017). Using click-chemistry for visualizing *in situ* changes of translational activity in planktonic marine bacteria. *Front. Microbiol.* 8. doi: 10.3389/fmicb.2017.02360

Levine, N. M., Toole, D. A., Neeley, A., Bates, N. R., Doney, S. C., and Dacey, J. W. H. (2016). Revising upper-ocean sulfur dynamics near Bermuda: New lessons from 3 years of concentration and rate measurements. *Environ. Chem.* 13, 302–313. doi: 10.1071/EN15045

Lidbury, I., Kröber, E., Zhang, Z., Zhu, Y., Murrell, J. C., Chen, Y., et al. (2016). A mechanism for bacterial transformations of DMS to DMSO: A missing link in the marine organic sulfur cycle. *Environ. Microbiol.* 18, 2754–2765. doi: 10.1111/1462-2920.13354

Linley, E. A. S., and Koop, K. (1986). Significance of pelagic bacteria as a trophic resource in a coral reef lagoon, one tree island, great barrier reef. *Mar. Biol.* 92, 457–464. doi: 10.1007/BF00392505

Liu, Y., Liu, C. Y., Yang, G. P., Zhang, H. H., and Zhang, S. H. (2016a). Biogeochemistry of dimethylsulfoniopropionate, dimethylsulfide and acrylic acid in the yellow Sea and the bohai Sea during autumn. *Environ. Chem.* 13, 127–139. doi: 10.1071/EN15025

Liu, X., Xiao, W. P., Landry, M. R., Chiang, K. P., Wang, L., and Huang, B. Q. (2016b). Responses of phytoplankton communities to environmental variability in the East China Sea. *Ecosystems* 19, 832–849. doi: 10.1007/s10021-016-9970-5

Lizotte, M., Levasseur, M., Law, C. S., Walker, C. F., Safi, K. A., Marriner, A., et al. (2017). Dimethylsulfoniopropionate (DMSP) and dimethylsulfide (DMS) cycling across contrasting biological hotspots of the new Zealand subtropical front. *Ocean Sci.* 13, 961–982. doi: 10.5194/os-13-961-2017

Lizotte, M., Levasseur, M., Michaud, S., Scarratt, M. G., Merzouk, A., Gosselin, M., et al. (2012). Macroscale patterns of the biological cycling of dimethylsulfoniopropionate (DMSP) and dimethylsulfide (DMS) in the Northwest Atlantic. *Biogeochemistry* 110, 183–200. doi: 10.1007/s10533-011-9698-4

Luce, M., Levasseur, M., Scarratt, M. G., Michaud, S., Royer, S.-J., Kiene, R., et al. (2011). Distribution and microbial metabolism of dimethylsulfoniopropionate and dimethylsulfide during the 2007 Arctic ice minimum. *J. Geophys. Res. C.* 116, C00G06. doi: 10.1029/2010JC006914

Masdeu-Navarro, M., Mangot, J.-F., Xue, L., Cabrera-Brufau, M., Gardner, S. G., Kieber, D. J., et al. (2022). Spatial and diel patterns of volatile organic compounds, DMSP-derived compounds, and planktonic microorganisms around a tropical scleractinian coral colony. *Front. Mar. Sci* 9, 944141. doi: 10.3389/fmars.2022.944141

Merzouk, A., Levasseur, M., Scarratt, M., Michaud, S., Lizotte, M., Rivkin, R. B., et al. (2008). Bacterial DMSP metabolism during the senescence of the spring diatom bloom in the Northwest Atlantic. *Mar. Ecol. Prog. Ser.* 369, 1–11. doi: 10.3354/meps07664

Merzouk, A., Levasseur, M., Scarratt, M. G., Michaud, S., Rivkin, R. B., Hale, M. S., et al. (2006). DMSP and DMS dynamics during a mesoscale iron fertilization experiment in the northeast pacific – part II: Biological cycling. *Deep-Sea Res. II* 53, 2370–2383. doi: 10.1016/j.dsr2.2006.05.022

Moneta, A., Veuger, B., van Rijswijk, P., Meysman, F., Soetaert, K., and Middelburg, J. J. (2014). Dissolved inorganic and organic nitrogen uptake in the coastal north Sea: A seasonal study. *Estuar. Coast. Shelf Sci.* 147, 78–86. doi: 10.1016/j.ecss.2014.05.022

Mopper, K., and Stahovec, W. L. (1986). Sources and sinks of low molecular weight organic carbonyl compounds in seawater. *Mar. Chem.* 19, 305–321. doi: 10.1016/0304-203(86)90052-6

Mopper, K., Zhou, X., Kieber, R. J., Kieber, D. J., Sikorski, R. J., and Jones, R. D. (1991). Photochemical degradation of dissolved organic carbon and its impact on the oceanic carbon cycle. *Nature* 353, 60–62. doi: 10.1038/353060a0

Moriarty, D. J. W., Pollard, P. C., and Hunt, W. G. (1985). Temporal and spatial variation in bacterial production in the water column over a coral reef. *Mar. Biol.* 85, 285–292. doi: 10.1007/BF00393249

Motard-Côté, J., Kieber, D. J., Rellinger, A., and Kiene, R. P. (2016). Influence of the Mississippi river plume and nonbioavailable DMSP on dissolved DMSP turnover in the northern gulf of Mexico. *Environ. Chem.* 13, 280–292. doi: 10.1071/EN15053

Motard-Côté, J., Levasseur, M., Scarratt, M. G., Michaud, S., Gratton, Y., Rivkin, R. B., et al. (2012). Distribution and metabolism of dimethylsulfoniopropionate (DMSP) and phylogenetic affiliation of DMSP-assimilating bacteria in northern Baffin Bay/Lancaster sound. *J. Geophys. Res. C.* 117, C00G11. doi: 10.1029/2011JC007330

Mulholland, M. R., and Lee, C. (2009). Peptide hydrolysis and the uptake of dipeptides by phytoplankton. *Limnol. Oceanogr.* 54, 856–868. doi: 10.4319/lo.2009.54.3.0856

Nakajima, R., Haas, A. F., Silveira, C. B., Kelly, E. L. A., Smith, J. E., Sandin, S., et al. (2018). Release of dissolved and particulate organic matter by the soft coral *Lobophytum* and subsequent microbial degradation. *J. Exp. Mar. Biol. Ecol.* 504, 53–60. doi: 10.1016/j.jembe.2018.02.008

Nakajima, R., Tanaka, Y., Guillemette, R., and Kurihara, H. (2017). Effects of coral-derived organic matter on the growth of bacterioplankton and heterotrophic nanoflagellates. *Coral Reefs* 36, 1171–1179. doi: 10.1007/s00338-017-1608-3

Nakajima, R., Yoshida, T., Azman, B. A. R., Zaleha, K., Othman, B. H. R., and Toda, T. (2009). *In situ* release of coral mucus by acropora and its influence on the heterotrophic bacteria. *Aquat. Ecol.* 43, 815–823. doi: 10.1007/s10452-008-9210-y

Nelson, C. E., Alldredge, A. L., McCliment, E. A., Amaral-Zettler, L. A., and Carlson, C. A. (2011). Depleted dissolved organic carbon and distinct planktonic bacterial communities in a rapid-flushing coral reef ecosystem. *ISME J.* 5, 1374–1387. doi: 10.1038/ismej.2011.12

Nelson, C. E., Donahue, M. J., Dulaiova, H., Goldberg, S. J., la Valle, F. F., Lubarsky, K., et al. (2015). Fluorescent dissolved organic matter as a multivariate biogeochemical tracer of submarine groundwater discharge in coral reef ecosystems. *Mar. Chem.* 177, 232–243. doi: 10.1016/j.marchem.2015.06.026

Olson, R. J., Zettler, E. R., and DuRand, M. D. (2018). "Phytoplankton analysis using flow cytometry," in *Handbook of methods in aquatic microbial ecology*. Eds. P. F. Kemp, B. F. Sherr, E. B. Sheer and J. J. Cole (Boca Raton, FL: Lewis Publishers), 175–186.

Patten, N. L., Wyatt, A. S. J., Lowe, R. J., and Waite, A. M. (2011). Uptake of picophytoplankton, bacterioplankton and virioplankton by a fringing coral reef community (Ningaloo reef, Australia). *Coral Reefs* 30, 555–567. doi: 10.1007/s00338-011-0777-8

Payet, J. P., McMinds, R., Burkepile, D. E., and Vega Thurber, R. L. (2014). Unprecedented evidence for high viral abundance and lytic activity in coral reef waters of the south pacific ocean. *Front. Microbiol.* 5. doi: 10.3389/fmicb.2014.00493

Pinhassi, J., Simó, R., González, J. M., Vila, M., Alonso-Sáez, L., Kiene, R. P., et al. (2005). Dimethylsulfoniopropionate turnover is linked to the composition and dynamics of the bacterioplankton assemblage during a microcosm phytoplankton bloom. *Appl. Environ. Microbiol.* 71, 7650–7660. doi: 10.1128/AEM.71.12.7650-7660.2005

Raina, J.-B., Dinsdale, E. A., Willis, B. L., and Bourne, D. G. (2010). Do the organic sulfur compounds DMSP and DMS drive coral microbial associations? *Trends Microbiol.* 18, 101–108. doi: 10.1016/j.tim.2009.12.002

Raina, J.-B., Tapiolas, D. M., Forêt, S., Lutz, A., Abrego, D., Ceh, J., et al. (2013). DMSP biosynthesis by an animal and its role in coral thermal stress response. *Nature* 502, 677–680. doi: 10.1038/nature12677

Rix, L. N., Burdett, H. L., and Kamenos, N. A. (2012). Irradiance-mediated dimethylsulphoniopropionate (DMSP) responses of red coralline algae. *Estuar. Coast. Shelf Sci.* 96, 268–272. doi: 10.1016/j.ecss.2011.11.022

Royer, S.-J., Levasseur, M., Lizotte, M., Arychuk, M., Scarratt, M. G., Wong, C. S., et al. (2010). Microbial dimethylsulfoniopropionate (DMSP) dynamics along a natural iron gradient in the northeast subarctic pacific. *Limnol. Oceanogr.* 55, 1614–1626. doi: 10.4319/lo.2010.55.4.1614

Ruiz-González, C., Simó, R., Sommaruga, R., and Gasol, J. M. (2013). Away from darkness: A review on the effects of solar radiation on heterotrophic bacterioplankton activity. *Front. Microbiol* 4, 131. doi: 10.3389/fmicb.2013.00131

Silveira, C. B., Cavalcanti, G. S., Walter, J. M., Silva-Lima, A. W., Dinsdale, E. A., Bourne, D. G., et al. (2017). Microbial processes driving coral reef organic carbon flow. *FEMS Microbiol. Rev.* 41, 575–595. doi: 10.1093/femsre/fux018

Simó, R., Archer, S. D., Pedrós-Alió, C., Gilpin, L., and Stelfox-Widdicombe, C. E. (2002). Coupled dynamics of dimethylsulfoniopropionate and dimethylsulfide cycling and the microbial food web in surface waters of the north Atlantic. *Limnol. Oceanogr.* 47, 53–61. doi: 10.4319/lo.2002.47.1.0053

Simó, R., Grimalt, J. O., and Albaigés, J. (1997). Dissolved dimethylsulphide, dimethylsulphoniopropionate and dimethylsulphoxide in western Mediterranean waters. *Deep Sea Res. II* 44, 929–950. doi: 10.1016/S0967-0645(96)00099-9

Simó, R., Vila-Costa, M., Alonso-Sáez, L., Cardelús, C., Guadayol, Ò., Vázquez-Domínguez, E., et al. (2009). Annual series of DMSP contribution to s and c fluxes through phytoplankton and bacterioplankton in a NW Mediterranean coastal site. *Aquat. Microb. Ecol.* 57, 43–55. doi: 10.3354/ame01325

Spielmeyer, A., and Pohnert, G. (2012). Daytime, growth phase and nitrate availability dependent variations of dimethylsulfoniopropionate in batch cultures of the diatom *Skeletonema marinoi*. *J. Exp. Mar. Biol. Ecol.* 413, 121–130. doi: 10.1016/j.jembe.2011.12.004

Spiese, C. E., Le, T., Zimmer, R. L., and Kieber, D. J. (2016). Dimethylsulfide membrane permeability, cellular concentrations and implications for physiological functions in marine algae. *J. Plankton Res.* 38, 41–54. doi: 10.1093/plankt/fbv106

Stefels, J., and van Leeuwe, M. A. (1998). Effects of iron and light stress on the biochemical composition of Antarctic *Phaeocystis* sp. (Prymnesiophyceae). i. intracellular DMSP concentrations. *J. Phycol.* 34, 486–495. doi: 10.1046/j.1529-8817.1998.340486.x

Steinke, M., Brading, P., Kerrison, P., Warner, M. E., and Suggett, D. J. (2011). Concentrations of dimethylsulfoniopropionate and dimethylsulfide are strain-specific in symbiotic dinoflagellates (*Symbiodinium* sp., *Dinophyceae*). *J. Phycol.* 47, 775–783. doi: 10.1111/j.1529-8817.2011.01011.x

Sunda, W. G., Hardison, R., Kiene, R. P., Bucciarelli, E., and Harada, H. (2007). The effect of nitrogen limitation on cellular DMSP and DMS release in marine phytoplankton: Climate feedback implications. *Aquat. Sci.* 69, 341–351. doi: 10.1007/s00027-007-0887-0

Sunda, W., Kieber, D. J., Kiene, R. P., and Huntsman, S. (2002). An antioxidant function for DMSP and DMS in marine algae. *Nature* 418, 317–320. doi: 10.1038/nature00851

Suttle, C. A., Chan, A. M., and Fuhrman, J. A. (1991). Dissolved free amino acids in the Sargasso Sea: Uptake and respiration rates, turnover times, and concentrations. *Mar. Ecol. Prog. Ser.* 70, 189–199. doi: 10.3354/meps070189

Swan, H. B., Deschaseaux, E. S. M., Jones, G. B., and Eyre, B. D. (2017). Quantification of dimethylsulphoniopropionate (DMSP) in *Acropora* spp. of reef building coral using mass spectrometry with deuterated internal standard. *Anal. Bioanal. Chem.* 409, 1929–1942. doi: 10.1007/s00216-016-0141-5

Takeda, K., Katoh, S., Mitsui, Y., Nakano, S., Nakatani, N., and Sakugawa, H. (2014). Spatial distributions of and diurnal variations in low molecular weight carbonyl compounds in coastal seawater, and the controlling factors. *Sci. Total Environ.* 493, 454–462. doi: 10.1016/j.scitotenv.2014.05.126

Taniguchi, A., Yoshida, T., and Eguchi, M. (2014). Bacterial production is enhanced by coral mucus in reef systems. *J. Exp. Mar. Bio. Ecol.* 461, 331–336. doi: 10.1016/j.jembe.2014.09.004

Tapiolas, D. M., Motti, C. A., Holloway, P., and Boyle, S. G. (2010). High levels of acrylate in the great barrier reef coral *Acropora millepora*. *Coral Reefs* 29, 621–625. doi: 10.1007/s00338-010-0608-3

Tapiolas, D. M., Raina, J.-B., Lutz, A., Willis, B. L., and Motti, C. A. (2013). Direct measurement of dimethysulfoniopropionate (DMSP) in reef-building corals using quantitative nuclear magnetic resonance (qNMR) spectroscopy. *J. Exp. Mar. Biol. Ecol.* 443, 85–89. doi: 10.1016/j.jembe.2013.02.037

Toole, D. A., Kieber, D. J., Kiene, R. P., Siegel, D. A., and Nelson, N. B. (2003). Photolysis and the dimethylsulfide (DMS) summer paradox in the Sargasso Sea. *Limnol. Oceanogr.* 48, 1088–1100. doi: 10.4319/lo.2003.48.3.1088

Tyssebotn, I. M. B. (2015). *An investigation of the marine acrylate cycle* (College of Environmental Science and Forestry. Syracuse, NY: Ph.D. thesis. State University of New York).

Tyssebotn, I. M. B., Kinsey, J. D., Kieber, D. J., Kiene, R. P., Rellinger, A. N., and Motard-Côté, J. (2017). Concentrations, biological uptake, and respiration of dissolved acrylate and dimethylsulfoxide in the northern gulf of Mexico. *Limnol. Oceanogr.* 62, 1198–1218. doi: 10.1002/lno.10495

Utermöhl, H. (1958). Zur vervollkommnung der quantitativen phytoplankton-methodik. *SIL Commun. 1953-1996* 9, 1–38. doi: 10.1080/05384680.1958.11904091

Van Alstyne, K. L., Schupp, P., and Slattery, M. (2006). The distribution of dimethylsulfoniopropionate in tropical pacific coral reef invertebrates. *Coral Reefs* 25, 321–327. doi: 10.1007/s00338-006-0114-9

Vila-Costa, M., Kiene, R. P., and Simó, R. (2008). Seasonal variability of the dynamics of dimethylated sulfur compounds in a coastal northwest Mediterranean site. *Limnol. Oceanogr.* 53, 198–211. doi: 10.4319/lo.2008.53.1.0198

Vila-Costa, M., Pinhassi, J., Alonso, C., Pernthaler, J., and Simó, R. (2007). An annual cycle of DMSP-sulfur assimilating bacterioplankton in the coastal NW Mediterranean. *Environ. Microbiol.* 9, 2451–2463. doi: 10.1111/j.1462-2920.2007.01363.x

Wegley, L., Edwards, R., Rodriguez-Brito, B., Liu, H., and Rohwer, F. (2007). Metagenomic analysis of the microbial community associated with the coral *Porites astreoides*. *Environ. Microbiol.* 9, 2707–2719. doi: 10.1111/j.1462-2920.2007.01383.x

Wheeler, P. A., Kirchman, D. L., Landry, M. R., and Kokklnakis, S. A. (1989). Diel periodicity in ammonium uptake and regeneration in the oceanic subarctic pacific: Implications for interactions in microbial food webs. *Limnol. Oceanogr.* 34, 1025–1033. doi: 10.4319/lo.1989.34.6.1025

Wikner, J., Rassoulzadegan, F., and Hagström, Å. (1990). Periodic bacterivore activity balances bacterial growth in the marine environment. *Limnol. Oceanogr.* 35, 313–324. doi: 10.4319/lo.1990.35.2.0313

Wild, C., Rasheed, M., Werner, U., Franke, U., Johnstone, R., and Huettel, M. (2004). Degradation and mineralization of coral mucus in reef environments. *Mar. Ecol. Prog. Ser.* 267, 159–171. doi: 10.3354/meps267159

Wu, X., Li, P.-F., Liu, C.-Y., Zhang, H.-H., Yang, G.-P., Zhang, S.-H., et al. (2017). Biogeochemistry of dimethylsulfide, dimethylsulfoniopropionate, and acrylic acid in the changjiang estuary and the East China Sea. *J. Geophys. Res. C.* 122, 10,245–10,261. doi: 10.1002/2017JC013265

Wu, X., Liu, C. Y., and Li, P. F. (2015). Photochemical transformation of acrylic acid in seawater. *Mar. Chem.* 170, 29–36. doi: 10.1016/j.marchem.2015.01.003

Wu, X., Li, P.-F., Zhang, H.-H., Zhu, M.-X., Liu, C.-Y., and Yang, G.-P. (2020). Acrylic acid and related dimethylated sulfur compounds in the bohai and yellow seas during summer and winter. *Biogeosci* 17, 1991–2008. doi: 10.5194/bg-17-1991-2020

Xue, L., and Kieber, D. J. (2021). Photochemical production and photolysis of acrylate in seawater. *Environ. Sci. Technol.* 55, 7135–7144. doi: 10.1021/acs.est.1c00327

Yost, D. M., Jones, R. J., and Mitchelmore, C. L. (2010). Alterations in dimethylsulphoniopropionate (DMSP) levels in the coral *Montastraea franksi* in response to copper exposure. *Aquat. Toxicol.* 98, 367–373. doi: 10.1016/j.aquatox.2010.03.005

Yost, D. M., and Mitchelmore, C. L. (2009). Dimethylsulphoniopropionate (DMSP) lyase activity in different strains of the symbiotic alga *Symbiodinium microadriaticum*. *Mar. Ecol. Prog. Ser.* 386, 61–70. doi: 10.3354/meps08031

Yost, D. M., and Mitchelmore, C. L. (2010). Determination of total and particulate dimethylsulphoniopropionate (DMSP) concentrations in four scleractinian coral species: A comparison of methods. *J. Exp. Mar. Biol. Ecol.* 395, 72–79. doi: 10.1016/j.jembe.2010.08.016

Zhou, X., and Mopper, K. (1997). Photochemical production of low-molecular-weight carbonyl compounds in seawater and surface microlayer and their air-sea exchange. *Mar. Chem.* 56, 201–213. doi: 10.1016/S0304-4203(96)00076-X

Zhu, Y., and Kieber, D. J. (2019). Concentrations and photochemistry of acetaldehyde, glyoxal, and methylglyoxal in the Northwest Atlantic ocean. *Environ. Sci. Technol.* 53, 9512–9521. doi: 10.1021/acs.est.9b01631

Zubkov, M. V., Fuchs, B. M., Archer, S. D., Kiene, R. P., Amann, R., and Burkill, P. H. (2002). Rapid turnover of dissolved DMS and DMSP by defined bacterioplankton communities in the stratified euphotic zone of the north Sea. *Deep-Sea Res. II* 49, 3017–3038. doi: 10.1016/S0967-0645(02)00069-3

Zweifel, U. L., Norrman, B., and Hagström, Å. (1993). Consumption of dissolved organic carbon by marine bacteria and demand for inorganic nutrients. *Mar. Ecol. Prog. Ser.* 101, 23–32. doi: 10.3354/meps101023